

Characterization of a Class A β -Lactamase from *Francisella tularensis* (Ftu-1) Belonging to a Unique Subclass toward Understanding AMR

Sourya Bhattacharya, Vivek Junghare, Mousumi Hazra, Niteesh Kumar Pandey, Abirlal Mukherjee, Kunal Dhankhar, Neeladrisingha Das, Partha Roy, Ramesh Chandra Dubey, and Saugata Hazra*

Cite This: *ACS Bio Med Chem Au* 2023, 3, 174–188

Read Online

ACCESS |

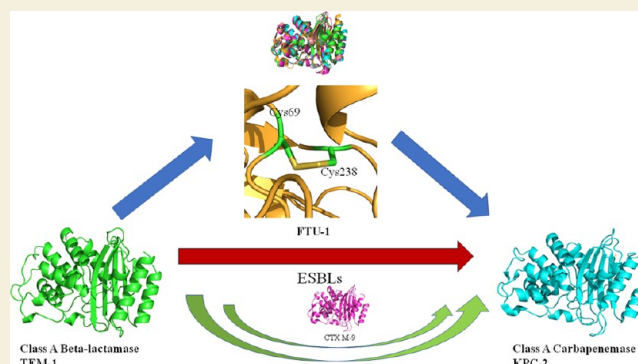
Metrics & More

Article Recommendations

Supporting Information

ABSTRACT: β -lactamase production with vast catalytic divergence in the pathogenic strain limits the antibiotic spectrum in the clinical environment. Class A carbapenemase shares significant sequence similarities, structural features, and common catalytic mechanisms although their resistance spectrum differs from class A β -lactamase in carbapenem and monobactam hydrolysis. In other words, it limited the antibiotic treatment option against infection, causing carbapenemase-producing superbugs. Ftu-1 is a class A β -lactamase expressed by the *Francisella tularensis* strain, a potent causative organism of tularemia. The chromosomally encoded class A β -lactamase shares two conserved cysteine residues, a common characteristic of a carbapenemase, and a distinctive class in the phylogenetic tree. Complete biochemical and biophysical characterization of the enzyme was performed to understand the overall stability and environmental requirements to perform optimally. To comprehend the enzyme–drug interaction and its profile toward various chemistries of β -lactam and β -lactamase inhibitors, comprehensive kinetic and thermodynamic analyses were conducted using various β -lactam drugs. The dynamic property of Ftu-1 β -lactamase was also predicted using molecular dynamics (MD) simulation to compare its loop flexibility and ligand binding with other related class A β -lactamases. Overall, this study fosters a comprehensive understanding of Ftu-1, proposed to be an intermediate class by characterizing its kinetic profiling, stability by biochemical and biophysical methodologies, and susceptibility profiling. This understanding would be beneficial for the design of new-generation therapeutics.

KEYWORDS: carbapenemase, catalytic divergence, superbugs, antimicrobial resistance (AMR), MD simulation, kinetic analysis, β -lactam



INTRODUCTION

Comparative T_m of Different Class A β -Lactamases. β -lactams are one of the most common antibiotics employed worldwide to treat bacterial infections.¹ β -lactam drugs introduced into clinical use against bacterial infection include penicillin, cephalosporins, monobactam, and carbapenems.² The introduction of β -lactam in clinical use causes the expression of a nonextended spectrum β -lactamase capable of hydrolyzing common β -lactams like penicillin and early-generation cephalosporin.³ The production of nonextended-spectrum β -lactamase causes the use of different higher-generation cephalosporins and β -lactamase inhibitors in clinics. Soon after introducing these β -lactams into the market, the nonextended-spectrum β -lactamase evolves as extended-spectrum (ESBLs) capable of hydrolyzing higher-generation penicillins and cephalosporins.^{4,5} After the continuous modification of β -lactamase, carbapenem derived from thienamycin was introduced as a last-resort treatment against bacterial infection expressing ESBLs.^{6,7} The commercial use of carbapenems worldwide causes carbapenem-resistant bacteria to show a different resistance mechanism.^{8,9} The main

resistance factor came from the enzyme carbapenemase, capable of hydrolyzing potent carbapenems and all known β -lactams.¹⁰ There are three subtypes of the enzyme carbapenemase. One is the serine-based class D β -lactamase of the OXA family,¹¹ while the other is the metal-dependent metallo β -lactamase.¹² Class A carbapenemase, the third kind, originated from class A β -lactamase due to a few changes that broadened their substrate specificity.¹³

There are a few class A carbapenemases like Nmca, SME, SFC-1, PenA, BIC-1, FPH-1, and SHV38 that were found to be chromosomally encoded; other types of carbapenemases like KPC, GES, and FRI-1 are plasmid-encoded; and IMI carbapenemase was found to be both plasmid-mediated and chromosomally encoded.¹⁴ Chromosomally mediated class A

Received: July 7, 2022

Revised: January 21, 2023

Accepted: January 25, 2023

Published: February 8, 2023



carbapenemases are generally found in some *Pseudomonas fluorescens*, *Serratia marcescens*, *Enterobacter cloacae*, *Serratia fonticola*, *Burkholderia cepacia*, *Francisella philomiragia*, and many others pathogenic organisms. Plasmid-mediated Class A carbapenemases like KPC and GES are generally expressed by clinically relevant organisms such as *Pseudomonas aeruginosa*, *Acinetobacter baumannii*, *Klebsiella pneumoniae*, and *Escherichia coli*.^{13,15} The emergence of class A carbapenemases in clinical concerning enterobacteriaceae isolates is a significant clinical concern because these clinical isolates can cause outbreaks such as a severe critical infection, nosocomial infection, and community-acquired infection with minimal antibacterial therapy.¹⁶ Like class A β -lactamase, class A carbapenemases also share conserved motifs like ⁷⁰SXXK⁷³, where X can be any amino acid, Ser₇₀ in the conserved motif is the acylating serine residues in β -lactamase-based catalysis, and Lys₇₃ is also a primary catalytic residue. ¹³⁰SDN¹³², Glu₁₆₆, ¹⁶⁶EXXXN¹⁷⁰, omega loop, and ²³⁴KTG²³⁶ motifs are similar to all of the class A carbapenemases. Class A carbapenemases have characteristic features like the presence of two conserved cysteine residues that form a disulfide linkage and connect two domains of the enzyme. This feature of disulfide bond formation is a notable exception in class A carbapenemases against class A serine β -lactamase. Here, in this paper, we focus on FtU-1, which is a Class A β -lactamase from *Francisella tularensis*. *F. tularensis* is well-known for tularemia disease. The β -lactamase FtU-1 has characteristic features of class A carbapenemase because it harbors two conserved cysteine residues at ambler positions 69 and 238 just before the catalytic serine residue and just after the conserved KTG motif. The detailed in silico analysis was performed to know the relatedness of this enzyme to other class A carbapenemases and β -lactamases.

Further, we characterized the enzyme by purifying and performing various biophysical and biochemical approaches. The catalytic diversity toward different generations of penicillin and cephalosporin was performed to understand the hydrolysis parameter of the protein. In detail, kinetics was performed with the help of a carbapenem to understand the carbapenemase activity of the enzyme. Inhibition spectra were determined to know the enzyme's behavior toward its inhibitor. Different biophysical approaches were used to study the enzyme stability and drug interaction parameter. Further, the effect of the enzyme directly in a cell harboring the gene was determined by observing the minimum inhibitory concentration (MIC) and fluorescence-based imaging. We characterized FtU-1 β -lactamase by interdisciplinary approaches combining in vitro and in silico methodologies.

MATERIALS AND METHODS

Evolutionary Analysis

Various class A β -lactamase sequences (mainly wild type from a different organism) were obtained from several databases like NCBI, BLDB,¹⁷ Uniprot, etc. After collecting all of the unique protein sequences of the class A β -lactamases, they were subjected to multiple-sequence alignment (MSA) with the help of clustal omega.¹⁸ Further evolutionary analysis was done with the help of the Maximum likelihood method. In the maximum likelihood method, amino acid substitution was performed using the JTT matrix.¹⁹ The closest neighbor for the ML heuristic technique was selected. The BioNJ and neighbor-join algorithms were employed to obtain an initial tree for heuristic search. Further analysis was carried out by molecular evolutionary genetics analysis (Mega X) software.²⁰

Molecular Dynamics (MD) Simulation

MD simulation of the apo FtU-1 protein was carried out using GROMACS 5.1.2²¹ TIP3P water model was implemented, and OPLS-AA was applied,^{22,23} all-atom force field with a LINUX environment. FtU-1 apo was modeled from the PDB structure 3P09 with residue numbers 20–287. The FtU-1 enzyme was solvated with the protein size dimension $8.17 \times 8.17 \times 8.17 \text{ nm}^3$ in a cubic box with a volume of 545.34 nm^3 and filled with SPC216 molecules of water. The total number of H₂O molecules was 16,406. Oppositely charged ions replaced solvent molecules to simulate the system at neutral pH. The numbers of Na⁺ and Cl⁻ ions were kept at 49 and 49 to counter the pH. A repeat cycle of 50,000 steps using the steepest energy minimization method (EM) was applied.²⁴ All of the systems were equilibrated before the final 100 ns simulation run. Relaxation times of 0.1 and 0.2 ps using an algorithm of Berendsen coupling were used following the maintaining of the isobaric and isothermal conditions using PBCs (periodic boundary conditions).²⁵ For all of the systems, the LINCS²⁶ algorithm was employed for fixing bond lengths with the help of a time step of 2 fs for these two systems. The PME (particle mesh Ewald)²⁷ method was utilized to measure the electrostatic interactions. A 1.0 nm cutoff was set to measure Coulombic interactions along with van der Waals interactions. The GROMACS package tool was used to analyze various MD simulation trajectories. Finally, Xmgrace, Pymol,^{28,29} and MATLAB³⁰ programs were utilized to compute and prepare high-resolution figures. The parameters like RMSF, RMSD, SASA, Rg, and H-bond were analyzed using VMD³¹ and Xmgrace to understand the thermal stability of FtU-1.

The MD simulation of apo and complex structures was done using GROMACS software version 2018.3 (www.gromacs.org). The ligand topology was prepared using ANTECHAMBER. The Amber ff99SB-ILDN force field and the TIP3P water model were used for the same. The explicit solvent was used for apo and complex structures at 300 K using a cubic box, keeping a distance of 1 nm from the protein. The system was neutralized by adding sodium and calcium ions. Energy minimization (EM) was performed using the conjugate gradient methods and the steepest descent. NVT and NPT equilibration was performed using the same configuration discussed earlier. The final MD run was performed for 100 ns for apo and complex structures. The analysis of MD was performed using GROMACS tools. VMD was used for the visualization of simulation trajectories. The graphs were plotted using Xmgrace software.

Protein Overexpression and Purification. A pMCSG7-based plasmid having the wild-type FtU-1 gene was used to overexpress and purify the desired protein. The cloned plasmid was transformed in the *E. coli* BL21(DE3) cells, and the expression of the protein was carried out by induction with 0.5 mM IPTG (isopropyl-D-1-thiogalactopyranoside) after attaining the absorbance of 0.6 at 600 nm (OD600). BL21 cells were incubated at 25 °C for 18 h; then, cells were collected and resuspended in 50 mM Tris buffer, having 250 mM NaCl, pH 7.5. Cells were disrupted with the help of sonication. The bacterial cell was sonicated using a probe sonicator from Helix Bioscience (India). With a power amplitude of 40%, the program was accomplished via a pulse on for 5 s, followed by a pulse off for 10 s. After centrifugation at 12,000 rpm, the supernatant was syringe-filtered through a 0.45-micron syringe filter. It was then poured into a Ni-NTA agarose column (the plasmid containing 6X His tagged for affinity chromatography) and eluted with a buffer having 50 mM Tris HCl, containing 250 mM imidazole and 250 mM sodium chloride at pH 7.5. The eluted fraction was collected and concentrated with the help of a protein concentrator of 10 kDa. The concentrated enzyme was loaded to the Sephadex G75 manual column for size exclusion chromatography. Purified protein was collected and visualized using 12% SDS-PAGE.

Circular Dichroism (CD) and Thermal Denaturation

Circular dichroism serves as an essential technique for the determination of secondary structural parameters of a protein molecule. Also, it helps in determining temperature and other denaturing-based stability measurements. A CD experiment also determines the fold of an enzyme or protein molecule and ligand

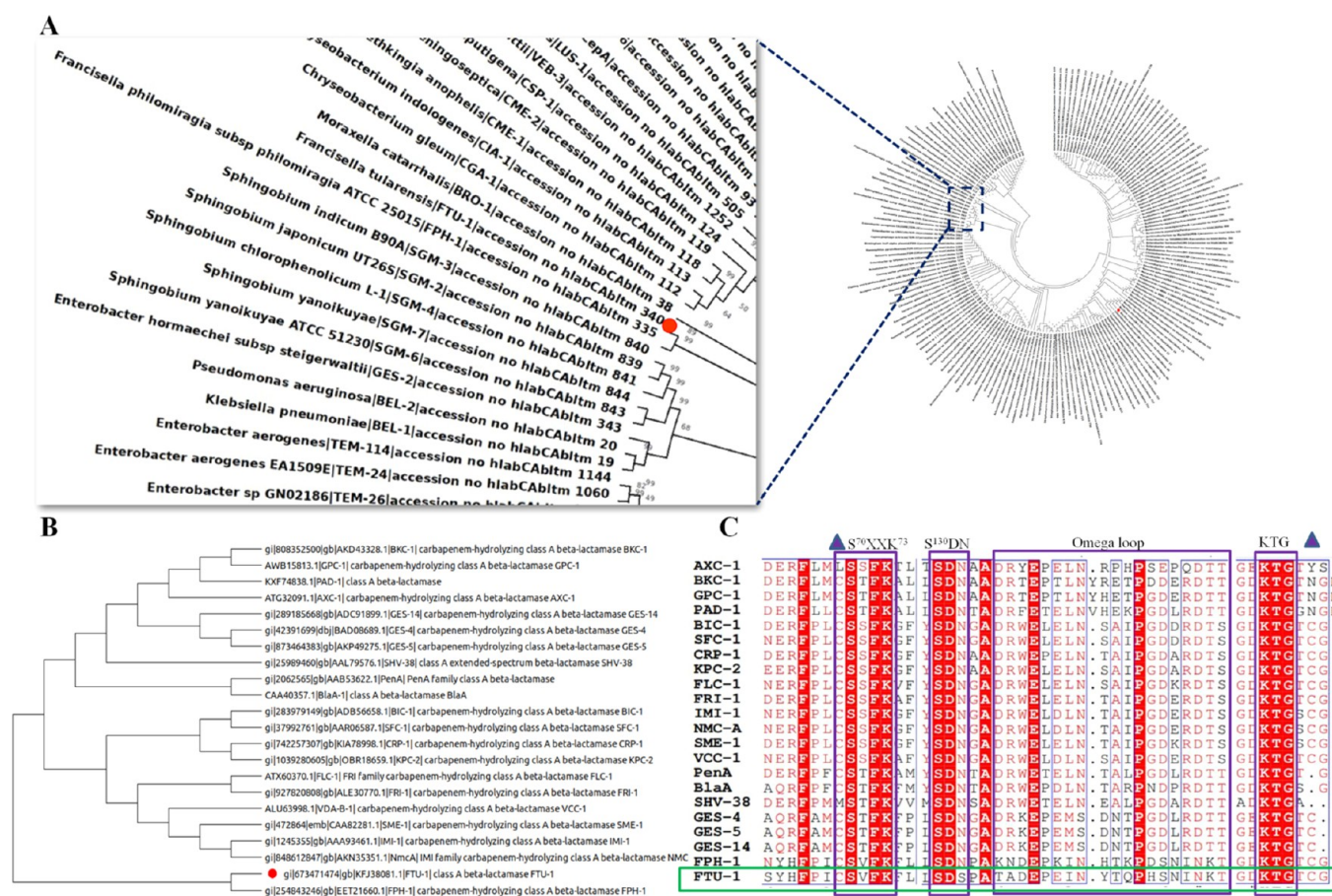


Figure 1. Sequence comparison and relatedness of Ftu-1 β -lactamase against class A β -lactamase and class A carbapenemase. (A) Evolutionary analysis of Ftu-1 with different class A β -lactamases. The Ftu-1 β -lactamase is highlighted with a red sphere in the zoomed picture. (B) Evolutionary analysis of Ftu-1 β -lactamase with different known class A carbapenemases. Ftu-1 is highlighted as a red sphere in the evolutionary tree of all class A carbapenemases. (C) Sequence comparison of all other class A carbapenemases from different species and Ftu-1, different conserved primary catalytic residues, motifs, and loops are highlighted with boxes, and the conserved cysteine is highlighted as a violet triangle in the multiple-sequence alignment picture.

binding secondary structural change associated with the complex. The CD experiment was done in a Jasco J-1500 spectrophotometer having a water Peltier-effect temperature system to maintain the temperature. Quartz glass cells having a path length of 0.1 cm were employed for the experiments. A total of 3.5 μ M Ftu-1 in 100 mM phosphate buffer was taken to monitor its secondary structure content from 190 to 260 nm in the far-ultraviolet (UV) spectra range, having a scan rate of 50 nm per minute.³² Thermal denaturation was carried out by taking the spectra of 3.5 μ M Ftu-1 in 100 mM phosphate buffer between 25 and 95 $^{\circ}$ C with a 5 $^{\circ}$ C/min interval. Ellipticity at 222 nm was plotted with temperature to analyze T_m (melting temperature).^{33,34} A total of 3.5 μ M was incubated with 1 mM DTT to break the disulfide bond and measured for melting the temperature determination by taking the CD spectra at different temperatures. The stability of Ftu-1 was determined by incubating 3.5 μ M Ftu-1 with urea concentrations ranging from 0.5 to 10 M; the denaturation by urea was obtained by monitoring the helical content at 222 nm.³⁵

Differential Scanning Calorimetry (DSC)

A DSC experiment to monitor the thermal stability was performed on a Microcal-VP-DSC (GE Healthcare). During the DSC experiment, the sample cell containing 70 μ M Ftu-1 was subjected to heating by increasing the temperature at a constant rate. The buffer thermal denaturation was taken as a blank and subjected to a baseline cancellation. Inbuilt origin software was used to analyze the graphs and other analyses.^{36,33,37}

Biochemical Characterization of Ftu-1 β -Lactamase

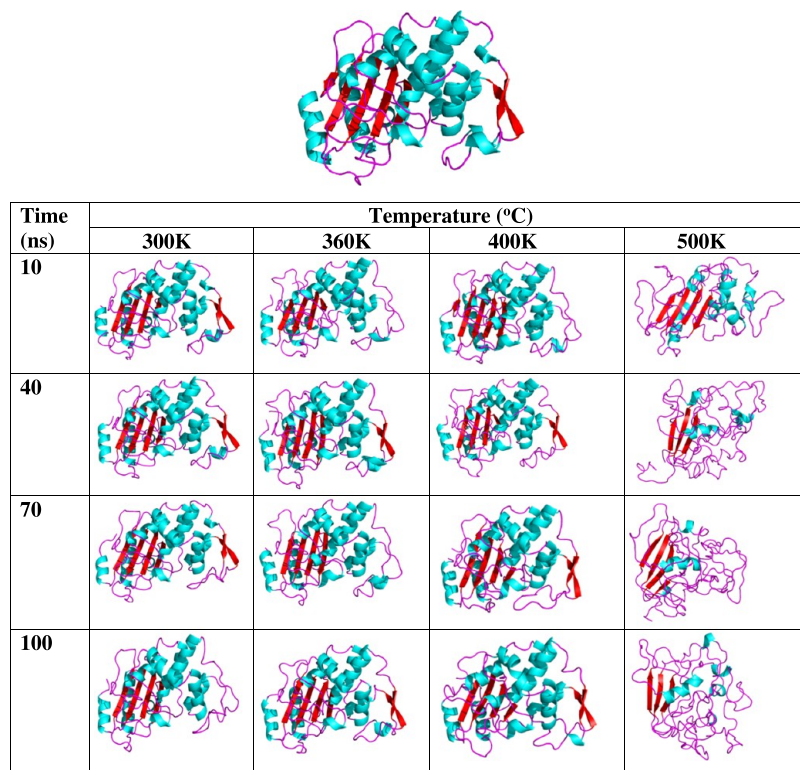
Steady-State Kinetics. A Cary 60 UV spectrophotometer was used for all of the kinetic analyses. The Ftu-1 was subjected to a buffer exchange by 50 mM PBS with pH 7.2 before starting the kinetic experiment.³⁸ All of the tested antibiotics were dissolved in phosphate buffer and were diluted to a working concentration of 1 mM. The enzyme kinetics were performed by different optimized substrate concentrations (100–1000 μ M).³⁹ The reaction was started by adding Ftu-1 (10 nM in the case of the penicillins and 1000–3000 nM for the cephalosporins). V_0 (the initial velocity) was calculated from the absorbance vs time graph and plotted against the substrate concentration to determine the enzyme kinetics parameters with the help of the Michaelis–Menten equation.⁴⁰

$$V = V_{\max} [S] / K_M + [S]$$

The enzyme turnover number k_{cat} was calculated as

$k_{\text{cat}} = V_{\max} / E_T$, where E_T is the final concentration of Ftu-1 used in the reaction mixture.

Temperature and pH Rate Profiling. As reporter substrates, nitrocefim was chosen for the temperature rate profiling experiment. The reaction mixture was prepared by taking a concentration gradient of nitrocefim from 20 to 120 μ M, and the reaction was begun by adding Ftu-1 at a concentration of 10 nM. The same reaction condition was followed for temperatures from 20 to 70 $^{\circ}$ C. All of the enzyme kinetics parameters were calculated as previously described in steady-state kinetics. The optimum temperature was observed by plotting the enzyme turnover number obtained at each temperature.

Table 1. Unfolding Pathway of Ftut-1 β -Lactamase^a

^aEach snapshot was taken from the different time frames of the MD simulation run at different temperatures.

Different buffer conditions were used to generate a pH spectrum starting from pH 3.7 to 10.5. For the pH-based study, Ftut-1 was incubated at these buffers overnight. CENTA was used for the pH-based kinetics study. The procedure for the reaction mixture and determination of enzyme kinetics parameters has been described previously in the steady-state kinetics procedure. Similar experiments were performed with a buffer containing different concentrations of NaCl to see the effect of salt in enzyme catalysis.^{33,37}

Inhibition Kinetics. MBIs (mechanism-based inhibitors) like sulbactam, clavulanic acid, and tazobactam, along with carbapenems like imipenem and meropenem, were used for the potential inhibitory assay against Ftut-1 β -lactamase. Then, 10 nM Ftut-1 was incubated with various inhibitors, and the reaction was started by adding 75 μ M nitrocefim as a reporter substrate. All of the reaction conditions were the same as previously described. All of the reactions were carried out for 20 min, and the time course of nitrocefim hydrolysis was recorded. The inhibitor dissociation constant (k_i) was calculated by measuring the hydrolysis of nitrocefim (reporter substrate) at different inhibitor concentrations (progress curve of nitrocefim hydrolysis) according to the equation⁴¹

$$\frac{v_t - v_{ss}}{v_0 - v_{ss}} = e^{-k_i(t)}$$

v_0 , v_t , and v_{ss} in the equation denote rates of hydrolysis of nitrocefim at times 0 and t and after the steady state has been established, respectively. The inhibitor dissociation constant for each inhibitor was calculated using the Dixon plot.^{42–45}

Molecular Docking with Substrates and Inhibitors. The knowledge-based approach was used to perform molecular docking of ampicillin, cephalothin, meropenem, carbenicillin, piperacillin, cefotaxime, imipenem, clavulanate, sulbactam, and tazobactam with Ftut-1. The substrate structures were manually prepared using ChemDraw 2D and Chem3D⁴⁶ software, and their energy minimization was performed using the MM2 method with the in-built tool of the same software. The Ftut-1 enzyme was modeled with the help of SWISS-MODEL software.⁴⁷ PDB id 3P09 was employed

as a template for this homology-based modeling. The resulting structure was energy-minimized using GROMACS tools using the methodology mentioned in the MD simulation part. Further, the substrate, enzyme, and grid preparation were done using AutoDock Tools v1.5.6.^{48,49} The grid was centered at (23.57, 71.75, 16.16) with dimensions on the x , y , and z -axis. Molecular docking was performed with the help of AutoDockVina for 10 modes. The based pose was selected using the lowest energy and orientation of carbonyl carbon fitting in the active site. PyMOL and COOT⁵⁰ were used for analysis.

Antimicrobial Susceptibility Testing and Live/Dead Cell Imaging. The disc diffusion method analyzed the resistance profile of control BL21 (DE3) and Ftut-1 clones. Antibiotic-coated discs (according to CLSI guidelines) were applied to the plates containing control and cloned bacteria. The results were interpreted by measuring the zone of inhibition.^{51–53} The MIC values of different antibiotics were tested against Ftut-1 gene-containing bacteria using microtiter broth dilution methods as previously described.^{33,54} Both the disk diffusion and microtiter broth dilution method utilized to understand the bacterial susceptibility were performed in duplicate. Fluorescence-based microscopy was implemented to understand the live/dead bacterial staining under the influence of different antibiotics. Acridine orange and EtBr stain were used to stain antibiotic-treated control and Ftut-1 gene-expressing bacteria. The staining and visualization were performed as described previously.⁴²

RESULTS

Sequence Comparison and Evolutionary Analysis to Understand the Relatedness of Ftut-1 β -Lactamase

The evolutionary analysis in Figure 1A exhibits the relationship among the assorted grouping of class A β -lactamases from diverse species. The evolutionary analysis also reveals the sequences of different genes bunched together, producing a significant basis for choosing the respective enzyme Ftut-1 in further detail. We found from the analysis that Ftut-1 β -

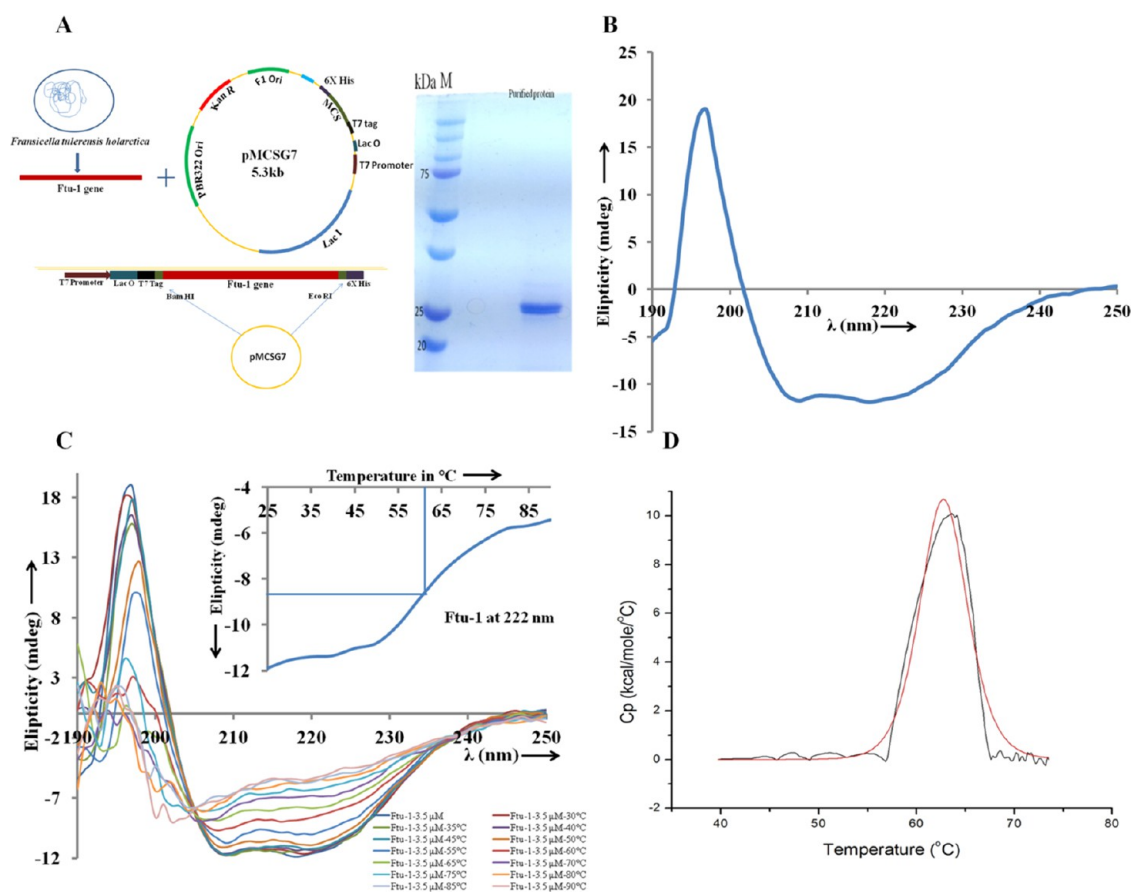


Figure 2. Purification and stability-based biophysical characterization of Ftut-1 β -lactamase. (A) Cloning and purification strategy of Ftut-1 β -lactamase; Ftut-1 was cloned in the pMCSG7 vector, and the purified Ftut-1 was visualized in SDS-PAGE. (B) CD spectra of Ftut-1 β -lactamase at a concentration of 3.5 μ M. (C) Thermal denaturation of Ftut-1 β -lactamase with the help of CD spectroscopy. CD spectra of 3.5 μ M Ftut-1 were collected at different temperatures, and the ellipticity at 222 nm was plotted against temperature to determine the melting temperature. (D) Thermal denaturation of Ftut-1 β -lactamase with the help of DSC.

lactamase (highlighted in the red sphere in Figure 1A) is related to FPH-1, a known carbapenemase from the *Francisella* species.⁵⁵ Ftut-1 is the immediate ancestor of BRO-1 β -lactamase from *Moraxella catarrhalis*. The most important observation is that Ftut-1 belongs to a completely distant class and falls into a distinct evolutionary tree branch. Ftut-1 is also related to a family of class A β -lactamase containing SGM, GES, and BEL; this family also includes narrow carbapenemase activity and is found to have a disulfide bond.^{56,57} When Ftut-1 was compared against all known class A carbapenemases, it was found that two enzymes from *Francisella* species, Ftut-1 (highlighted in the red sphere in Figure 1B) and FPH-1, represent a distinct class in the evolutionary tree. Detailed sequence analysis of Ftut-1 with other known carbapenemases shows that primary catalytic residues, conserved motifs, and loops are similar in Ftut-1 (Figure 1C). The MSA study compares various motifs like S⁷⁰XXX⁷³ and K²³⁴T/SG²³⁶ motifs found preserved for the Ftut-1 β -lactamase to the other class A carbapenemases. Two motifs, S¹³⁰DN¹³² and omega loop, along with the critical residues involved in catalysis like Arg164, Asp163, Glu166, Leu169, and Asn170 (present in the enzyme's omega loop), show high preservation compared with the rest of the other class A carbapenemases. The two conserved cysteine residues at positions 69 and 238 are also present in Ftut-1. These two residues also form the characteristics of the disulfide bond in the three-dimensional modeled

structure. All of the critical residues and motifs are highlighted in Figure 1C and represent the three-dimensional structure of Ftut-1 in Figure S1.

Biophysical and Dynamic Characterization of Ftut-1 β -Lactamase Focusing on Enzyme Stability

Overall Stability, Structural Flexibility, and Compactness of Ftut-1 Using MD Simulation. A protein molecule unfolds to its denatured form under various denaturing conditions. The influence of temperature is one of the key factors for unfolding protein molecules. Apo Ftut-1 is subjected to MD simulation run at various temperatures like 300, 320, 340, 360, 400, and 500 K. These simulations mimic the denaturation or stability assessment via various experimental techniques and correlate these two. In general, in a complete simulation run of several nanoseconds, we can see various conformations of a protein molecule at different time scales. Here, Ftut-1 was tested against various temperatures from 300 to 500 K. We observed various conformations at different time intervals of each simulation run at various temperatures (10 snapshots in each 100 ns simulation run in an interval of 10 ns). We observed that Ftut-1 shows significant thermal stability. The Ftut-1 core structure remains stable at 360 K. Up to 360 K, there is no significant change in the secondary structure content as per visualization of the Ftut-1 snapshots at each temperature. We describe the pictorial demonstration of the unfolding of Ftut-1 β -lactamase in Tables 1 and S1. For better

Table 2. Temperature Rate Profiling of Ftut-1 β -Lactamase^a

temperature in °C	K_M (μM)	V_{max} ($\mu\text{M}/\text{min}$)	k_{cat} (min^{-1})	k_{cat}/K_M ($\mu\text{M}^{-1} \text{min}^{-1}$)
20	83.6 \pm 29.38	21.55 \pm 2.6	2155 \pm 265	28.13 \pm 6.7
30	100.86 \pm 50.86	33.61 \pm 4.55	3361 \pm 455	41.345 \pm 16.10
40	211 \pm 62.13	55.27 \pm 4.25	5527 \pm 425	27.89 \pm 6.17
50	33.47 \pm 0.96	7.9 \pm 0.86	790.5 \pm 86.5	23.7 \pm 3.26
60	256.94 \pm 3.6	1.45 \pm 0.1	145 \pm 9.5	0.56 \pm 0.01
70	263.8 \pm 6.5	1.135 \pm 0.2	113.5 \pm 8.0	0.43 \pm 0.08

^aThe kinetic reaction was carried out at different temperatures with the help of a fixed substrate concentration of nitrocefin 20–120 μM (A chromogenic cephalosporin) and an Ftut-1 concentration of 10 nM.

subatomic-level analysis, we performed RMSD by taking the characteristic structure of Ftut-1 β -lactamase. The thermal stability of Ftut-1 at various temperatures can be looked at utilizing RMSD because RMSD is the distinction between the backbones of the protein, compared with their beginning structure, all through a simulation run. We measure the RMSD of simulated Ftut-1 at several temperatures (Figure S2A).

Higher RMSD means more deviation in the protein backbone and hence a less stabilized structure. We calculated the average RMSD values of simulated Ftut-1 at various temperatures and observed that the least average RMSD value at 320 K is 0.2042 nm, the most stabilized structure. Ftut-1 has average RMSD values of 0.2788 and 0.2746 nm, respectively, at 340 and 360 K, which suggests that the Ftut-1 stability decreases at this temperature and remains stable at these two temperatures. Average RMSD values increase from 0.2834 to 1.19 nm from 400 to 500 K, suggesting complete denaturation. Side-chain residue flexibility and stability can also be seen by RMSF analysis (Figure S2B). From the MD simulation trajectories of Ftut-1 at various temperatures, we observed that the average RMSF value increases significantly with an increase in temperature.

We found that the average RMSD values of 300, 320, 340, 360, 400, and 500 K are 0.1178, 0.1461, 0.1595, 0.1734, 0.2068, and 0.8012 nm, respectively. The increase in average RMSF value indicates that structural flexibility increases with temperature, decreasing the stability. The radius of gyration also provides information on the compactness of a protein molecule. The radius of gyration describes the difference between the RMS distances of the atoms to the center of gravity. More values in a radius of gyration mean a less stable structure (Figure S2C). We observe that the average R_g value did not show significant differences at higher temperatures. Only at 500 K, we observed significant differences in the average R_g value of 1.91 nm.

When a protein molecule denatures under the influence of temperature, its respective SASA value also increases because gradual denaturation will cause exposure of the hydrophobic core to the solvent, increasing the SASA value. We calculated the SASA value of Ftut-1 at 300, 320, 340, 360, 400, and 500 K (Figure S2D). We also observed the system's average hydrogen bond between a protein and a water molecule (Figure S2E). We have tested the hydrogen bond with a distant cutoff of 0.35 nm. More hydrogen bonds directly correlate with the stability of a protein molecule. We observed that the average number of hydrogen bonds decreases as the temperature increases. We observed the highest average hydrogen bond of 557 at 300 K. The average hydrogen bond decreases to 436 and 332 at 400 and 500 K, respectively, suggesting unfolding under the influence of temperature.

Protein Overexpression and Purification. The Ftut-1 gene was subjected to cloning to the plasmid pMCSG7. The enzyme was first purified by Ni-NTA chromatography. Ftut-1 was then subjected to gel filtration using the Sephadex G75. The characteristic band at 32 kDa suggests the final purification of the Ftut-1 enzyme (Figure 2A). The purified Ftut-1 was utilized for additional biochemical and biophysical characterizations.

Thermal Denaturation Comparison Using Differential Scanning Calorimetry and Circular Dichroism Spectroscopy. A total of 3.5 μM Ftut-1 was monitored for helical content and scanned at far-UV spectra in the 190–250 nm range. The CD spectrum of Ftut-1 is depicted in Figure 2B. The CD spectrum shows two significant peaks for the helical protein. The melting temperature was determined by measuring the CD spectrum at an increasing temperature between 25 and 90 °C having a heating rate of 5 C/min. The ellipticity obtained at 222 nm from each range from 20 to 90 °C was plotted against temperature to obtain the melting temperature (Figure 2C). We have plotted the data and found that the melting temperature is around 63 °C for Ftut-1. The melting temperature of Ftut-1 is significantly higher than those of other tested class A β -lactamases like TEM, Bla1, and BEL. The significant increase in melting temperature may be associated with the disulfide bond present in the protein. We used 1 mM DTT to break the disulfide bond. Ftut-1 (3.5 μM) was incubated in 1 mM DTT, and spectra were collected at the same temperature range. We found that the melting temperature decreased by around 2–3 °C (Figure S3A). The same decline in T_m was observed when the urea concentration was increased to the Ftut-1 protein. It was then plotted against ellipticity at 222 nm and urea concentration. The data analysis showed that the denaturation concentration of urea toward Ftut-1 is 6 M (Figure S3B). DSC can best characterize the stability of the protein in its native three-dimensional (3D) form. In DSC, a protein's thermal denaturation is related to the change in heat when the protein is heated at a constant rate. DSC can also measure the enthalpy related to the unfolding of a protein molecule when it denatures because of the heat. Through the differential scanning calorimetry experiment, we can also calculate the heat capacity (ΔC_p) for the denaturation of the protein under the influence of heat (Figure 2D). This data obtained from the differential scanning calorimetry curve provided information on enzyme stability with thermal denaturation because of the absorption of heat by the various noncovalent and covalent bonds in the protein. From the differential scanning calorimetry curve, we observed the T_m of Ftut-1 at around 63 °C (Figure 2D).

Temperature, pH, and Salt-Based Rate Profiling Using Kinetic Analysis. Nitrocefin was used as a chromogenic reporter substrate for hydrolysis analysis of Ftut-

Table 3. pH Rate Profiling of Ftu-1 β -Lactamase^a

pH	K_M (μM)	V_{max} ($\mu\text{M} / \text{min}$)	k_{cat} (min^{-1})	k_{cat}/K_M ($\mu\text{M}^{-1} \text{min}^{-1}$)
3.7	67.3 \pm 37.4	0.180 \pm 0.05	18.45 \pm 3.55	0.36 \pm 0.14
4.8	654.8 \pm 37.08	1.001 \pm 0.005	101 \pm 1	0.152 \pm 0.009
5.8	65 \pm 8	13.12 \pm 0.62	1312.75 \pm 62.75	20.37 \pm 1.54
6.4	89 \pm 5	24.8 \pm 0.9	2309.4 \pm 134.3	27.32 \pm 0.20
7.2	37.38 \pm 1.43	30.5 \pm 0.5	3049 \pm 54.79	81.63 \pm 1.63
7.6	128.42 \pm 57	49.51 \pm 15.84	4951.67 \pm 1583	41.36 \pm 6.25
8.5	227.63 \pm 11.13	25.75 \pm 2.1	2575 \pm 217.5	11.2 \pm 0.39
9.5	53.57 \pm 4.4	0.38 \pm 0.1	38.96 \pm 11.2	1.43 \pm 0.8
10.5	218.5 \pm 30.8	0.088 \pm 0.0015	8.85 \pm 0.15	0.041 \pm 0.005

^aThe ftu-1 enzyme was incubated at various pHs, and the kinetics runs were performed using CENTA as the reporter substrate in the concentration range of 20–100 μM .

Table 4. Steady-State Kinetic Parameters (β -Lactam Hydrolysis Efficiencies) of Ftu-1 β -Lactamase toward Different Generations of β -Lactam Antibiotics

antimicrobials	generation	K_M (μM)	k_{cat} (S^{-1})	k_{cat}/K_M ($\text{M}^{-1} \text{S}^{-1}$)
nitrocefin	chromogenic cephalosporin	153 \pm 8	33.5 \pm 2.5	(0.22 \pm 0.005) $\times 10^6$
penicillin G	amino penicillin	836 \pm 32	833 \pm 50	(1 \pm 0.02) $\times 10^6$
ampicillin	amino penicillin	547 \pm 15	832 \pm 33.5	(1.52 \pm 0.02) $\times 10^6$
carbenicillin	carboxy penicillin	561 \pm 40	275 \pm 17	(0.49 \pm 0.005) $\times 10^6$
oxacillin	β -lactamase resistant	105 \pm 3	59 \pm 2	(5.6 \pm 0.05) $\times 10^5$
piperacillin	ureido penicillin	231 \pm 8	525 \pm 25	(2.27 \pm 0.03) $\times 10^6$
cephalothin	1st-gen cephalosporin	17 \pm 1	0.03 \pm 0.2	(2.0 \pm 0.01) $\times 10^3$
cefalexin	1st-gen cephalosporin	37 \pm 3	0.04 \pm 1	(1.0 \pm 0.01) $\times 10^3$
CENTA	chromogenic cephalosporin	37.38 \pm 1.43	50.81 \pm 0.91	(1.36 \pm 0.03) $\times 10^6$
cefuroxime ^a	2nd-gen cephalosporin	14 \pm 2	0.010 \pm 0.001	(7.1 \pm 0.1) $\times 10^2$
ceftazidime ^a	3rd-gen cephalosporin	55 \pm 7	0.022 \pm 0.001	(4.0 \pm 0.6) $\times 10^2$
imipenem ^a	carbapenem	31 \pm 4	0.017 \pm 0.001	(5.2 \pm 0.8) $\times 10^2$
meropenem ^a	carbapenem	≥ 100	ND ^b	(2.5 \pm 0.3) $\times 10^2$
doripenem ^a	carbapenem	≥ 100	ND ^b	(2.1 \pm 0.1) $\times 10^2$

^aAntunes et al., 2012. ^bND, Not detected.

1 β -lactamase at various temperatures. Kinetic assays were monitored at a temperature starting from 20 to 70 $^{\circ}\text{C}$. All of the enzymatic parameters at different temperatures are depicted in Table 2. The highest enzyme efficiency was observed at 30 $^{\circ}\text{C}$ temperature with a k_{cat}/K_M of $41.345 \pm 16.10 \mu\text{M}^{-1} \text{min}^{-1}$. We have marked significant catalytic efficiency up to 50 $^{\circ}\text{C}$ with a k_{cat}/K_M of $23.7 \pm 3.26 \mu\text{M}^{-1} \text{min}^{-1}$. The enzyme activity drastically decreases above this temperature. The k_{cat}/K_M obtained from each temperature was plotted against temperature to understand the optimum temperature for catalysis (Figure S3C)

Another chromogenic reporter substrate CENTA was used in the enzyme assay at various pH values to understand the pH dependence in enzyme catalysis. The kinetic analysis was monitored in the pH range from 3.7 to 10.5. We have observed that Ftu-1 is enzymatically the most active in pH 7.2 and 7.6 with k_{cat}/K_M values of 81.63 ± 1.63 and $41.36 \pm 6.25 \mu\text{M}^{-1} \text{min}^{-1}$, respectively (Table 3). At pH 5.8 and 6.4, Centa hydrolysis was also obtained with k_{cat}/K_M values of 20.37 ± 1.54 and $27.32 \pm 0.20 \mu\text{M}^{-1} \text{min}^{-1}$. The enzyme efficiency was significantly less at lower pHs like 3.7 and 4.8, and the same decrease in enzyme efficiency was also observed at higher pHs. The k_{cat}/K_M obtained at various pHs was plotted with increasing pH to obtain the optimum pH for enzyme catalysis (Figure S3D).

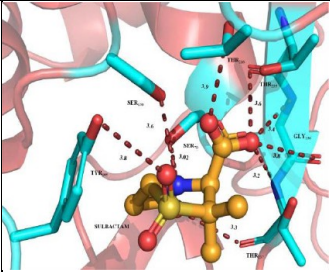
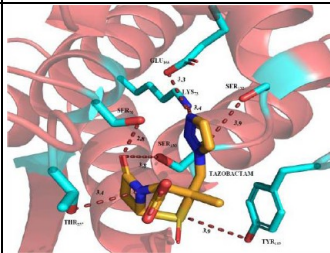
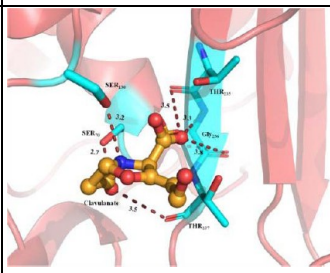
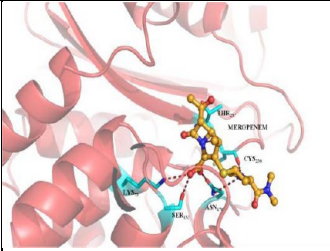
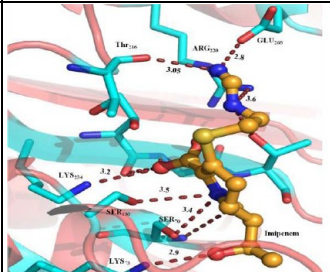
Buffer containing different concentrations of NaCl was also screened. We observed that Ftu-1 could hydrolyze ampicillin (used as the reporter substrate) efficiently at a NaCl

concentration of 500 mM, drastically decreasing above this concentration. However, no significant difference in enzyme efficiency was observed in the case of increasing the salt concentration from 0 to 2 M. All of the enzyme kinetic parameters are tabulated in Table S2.

Biochemical and Interaction Studies of Ftu-1 with Different Substrates and Inhibitors. Steady-State Kinetics to Understand the Hydrolysis Spectrum. Different generations of β -lactam antimicrobials were tested against Ftu-1 to understand the hydrolysis potential of Ftu-1 against these antibiotics. From the enzyme kinetics parameter in Table 4, narrow-generation penicillins like ampicillin and penicillin G were readily hydrolyzed by Ftu-1 with k_{cat}/K_M on the orders of 1 ± 0.02 and $1.52 \pm 0.02 \mu\text{M}^{-1} \text{s}^{-1}$. Carbenicillin and oxacillin are comparatively less hydrolyzed as compared to penicillin and ampicillin. Interestingly, piperacillin, a higher-generation penicillin, hydrolyzed more strongly by Ftu-1 with a k_{cat}/K_M on the order of $2.27 \pm 0.03 \mu\text{M}^{-1} \text{s}^{-1}$. Ftu-1 is active only against first-generation cephalosporin with lower k_{cat}/K_M values of 0.002 ± 0.005 and $0.001 \pm 0.001 \mu\text{M}^{-1} \text{s}^{-1}$ against cephalothin and cefalexin. Another study also found that higher-generation cephalosporin like cefoxitin, cepharmycin, and monobactam like aztreonam remain unhydrolyzed in the presence of Ftu-1;⁵⁷ this previous study also demonstrated that Ftu-1 can hydrolyze carbapenem with a lower hydrolyzing efficiency.⁵⁷

Inhibitor Kinetics to Understand the Inhibitory Potential of Different MBIs and Carbapenems. We have analyzed the inhibition kinetics with mechanism-based inhibitors against

Table 5. Inhibition Kinetics Profiling of MBIs (Sulbactam, Tazobactam, and Clavulanate) and Carbapenems (Meropenem and Imipenem) against Ftu-1 β -Lactamase

Protein Name	Inhibitors name	K _i (μ M)	Molecular docking	Interaction details																																																												
Ftu-1	Sulbactam	21.12	 <p>Binding Energy = -6.4 kcal/mol</p>	<table border="1"> <thead> <tr> <th>Ligand</th> <th>Atom Name</th> <th>Residue Name</th> <th>Residue No</th> <th>Atom Name</th> <th>Distance (in Å)</th> </tr> </thead> <tbody> <tr> <td>SUL</td> <td>O11</td> <td>THR</td> <td>237</td> <td>O</td> <td>3.3</td> </tr> <tr> <td>SUL</td> <td>O13</td> <td>TYR</td> <td>105</td> <td>OH</td> <td>3.8</td> </tr> <tr> <td>SUL</td> <td>O10</td> <td>THR</td> <td>237</td> <td>N</td> <td>3.2</td> </tr> <tr> <td>SUL</td> <td>O10</td> <td>THR</td> <td>235</td> <td>O</td> <td>3.6</td> </tr> <tr> <td>SUL</td> <td>O10</td> <td>GLY</td> <td>236</td> <td>N</td> <td>3.4</td> </tr> <tr> <td>SUL</td> <td>O11</td> <td>SER</td> <td>70</td> <td>OG</td> <td>3.02</td> </tr> <tr> <td>SUL</td> <td>O9</td> <td>SER</td> <td>130</td> <td>OG</td> <td>3.6</td> </tr> </tbody> </table>	Ligand	Atom Name	Residue Name	Residue No	Atom Name	Distance (in Å)	SUL	O11	THR	237	O	3.3	SUL	O13	TYR	105	OH	3.8	SUL	O10	THR	237	N	3.2	SUL	O10	THR	235	O	3.6	SUL	O10	GLY	236	N	3.4	SUL	O11	SER	70	OG	3.02	SUL	O9	SER	130	OG	3.6												
Ligand	Atom Name	Residue Name	Residue No	Atom Name	Distance (in Å)																																																											
SUL	O11	THR	237	O	3.3																																																											
SUL	O13	TYR	105	OH	3.8																																																											
SUL	O10	THR	237	N	3.2																																																											
SUL	O10	THR	235	O	3.6																																																											
SUL	O10	GLY	236	N	3.4																																																											
SUL	O11	SER	70	OG	3.02																																																											
SUL	O9	SER	130	OG	3.6																																																											
Ftu-1	Tazobactam	1.1968	 <p>Binding Energy = -6.6 kcal/mol</p>	<table border="1"> <thead> <tr> <th>Ligand</th> <th>Atom Name</th> <th>Residue Name</th> <th>Residue No</th> <th>Atom Name</th> <th>Distance (in Å)</th> </tr> </thead> <tbody> <tr> <td>TAZO</td> <td>O13</td> <td>TYR</td> <td>105</td> <td>OH</td> <td>3.9</td> </tr> <tr> <td>TAZO</td> <td>N16</td> <td>SER</td> <td>132</td> <td>OG</td> <td>3.9</td> </tr> <tr> <td>TAZO</td> <td>N18</td> <td>LYS</td> <td>73</td> <td>NZ</td> <td>3.4</td> </tr> <tr> <td>TAZO</td> <td>N18</td> <td>GLU</td> <td>166</td> <td>OE2</td> <td>3.3</td> </tr> <tr> <td>TAZO</td> <td>N16</td> <td>SER</td> <td>130</td> <td>OG</td> <td>3.8</td> </tr> <tr> <td>TAZO</td> <td>N18</td> <td>SER</td> <td>70</td> <td>OG</td> <td>2.8</td> </tr> <tr> <td>TAZO</td> <td>N18</td> <td>THR</td> <td>237</td> <td>O</td> <td>3.4</td> </tr> </tbody> </table>	Ligand	Atom Name	Residue Name	Residue No	Atom Name	Distance (in Å)	TAZO	O13	TYR	105	OH	3.9	TAZO	N16	SER	132	OG	3.9	TAZO	N18	LYS	73	NZ	3.4	TAZO	N18	GLU	166	OE2	3.3	TAZO	N16	SER	130	OG	3.8	TAZO	N18	SER	70	OG	2.8	TAZO	N18	THR	237	O	3.4												
Ligand	Atom Name	Residue Name	Residue No	Atom Name	Distance (in Å)																																																											
TAZO	O13	TYR	105	OH	3.9																																																											
TAZO	N16	SER	132	OG	3.9																																																											
TAZO	N18	LYS	73	NZ	3.4																																																											
TAZO	N18	GLU	166	OE2	3.3																																																											
TAZO	N16	SER	130	OG	3.8																																																											
TAZO	N18	SER	70	OG	2.8																																																											
TAZO	N18	THR	237	O	3.4																																																											
Ftu-1	Clavulanate	30.68	 <p>Binding Energy = -5.7 kcal/mol</p>	<table border="1"> <thead> <tr> <th>Ligand</th> <th>Atom Name</th> <th>Residue Name</th> <th>Residue No</th> <th>Atom Name</th> <th>Distance (in Å)</th> </tr> </thead> <tbody> <tr> <td>CLAV</td> <td>O4</td> <td>SER</td> <td>70</td> <td>OG</td> <td>2.7</td> </tr> <tr> <td>CLAV</td> <td>O4</td> <td>THR</td> <td>237</td> <td>O</td> <td>3.5</td> </tr> <tr> <td>CLAV</td> <td>O6</td> <td>GLY</td> <td>236</td> <td>O</td> <td>3.8</td> </tr> <tr> <td>CLAV</td> <td>O6</td> <td>THR</td> <td>235</td> <td>O</td> <td>3.5</td> </tr> <tr> <td>CLAV</td> <td>O4</td> <td>SER</td> <td>130</td> <td>O</td> <td>3.2</td> </tr> <tr> <td>CLAV</td> <td>O6</td> <td>GLY</td> <td>236</td> <td>N</td> <td>3.3</td> </tr> </tbody> </table>	Ligand	Atom Name	Residue Name	Residue No	Atom Name	Distance (in Å)	CLAV	O4	SER	70	OG	2.7	CLAV	O4	THR	237	O	3.5	CLAV	O6	GLY	236	O	3.8	CLAV	O6	THR	235	O	3.5	CLAV	O4	SER	130	O	3.2	CLAV	O6	GLY	236	N	3.3																		
Ligand	Atom Name	Residue Name	Residue No	Atom Name	Distance (in Å)																																																											
CLAV	O4	SER	70	OG	2.7																																																											
CLAV	O4	THR	237	O	3.5																																																											
CLAV	O6	GLY	236	O	3.8																																																											
CLAV	O6	THR	235	O	3.5																																																											
CLAV	O4	SER	130	O	3.2																																																											
CLAV	O6	GLY	236	N	3.3																																																											
Ftu-1	Meropenem	1.53	 <p>Binding Energy = -6.9 kcal/mol</p>	<table border="1"> <thead> <tr> <th>Ligand</th> <th>Atom Name</th> <th>Residue Name</th> <th>Residue No</th> <th>Atom Name</th> <th>Distance (in Å)</th> </tr> </thead> <tbody> <tr> <td>MRP</td> <td>N1</td> <td>THR</td> <td>237</td> <td>O</td> <td>3.8</td> </tr> <tr> <td>MRP</td> <td>N2</td> <td>CYS</td> <td>238</td> <td>O</td> <td>2.8</td> </tr> <tr> <td>MRP</td> <td>N2</td> <td>ASN</td> <td>170</td> <td>ND2</td> <td>3.8</td> </tr> <tr> <td>MRP</td> <td>O23</td> <td>ASN</td> <td>170</td> <td>OD1</td> <td>3.3</td> </tr> <tr> <td>MRP</td> <td>O24</td> <td>LYS</td> <td>73</td> <td>NZ</td> <td>3.0</td> </tr> <tr> <td>MRP</td> <td>O24</td> <td>SER</td> <td>132</td> <td>OG</td> <td>2.7</td> </tr> </tbody> </table>	Ligand	Atom Name	Residue Name	Residue No	Atom Name	Distance (in Å)	MRP	N1	THR	237	O	3.8	MRP	N2	CYS	238	O	2.8	MRP	N2	ASN	170	ND2	3.8	MRP	O23	ASN	170	OD1	3.3	MRP	O24	LYS	73	NZ	3.0	MRP	O24	SER	132	OG	2.7																		
Ligand	Atom Name	Residue Name	Residue No	Atom Name	Distance (in Å)																																																											
MRP	N1	THR	237	O	3.8																																																											
MRP	N2	CYS	238	O	2.8																																																											
MRP	N2	ASN	170	ND2	3.8																																																											
MRP	O23	ASN	170	OD1	3.3																																																											
MRP	O24	LYS	73	NZ	3.0																																																											
MRP	O24	SER	132	OG	2.7																																																											
	Imipenem	73.76	 <p>Binding Energy = -6.4 kcal/mol</p>	<table border="1"> <thead> <tr> <th>Ligand</th> <th>Atom Name</th> <th>Residue Name</th> <th>Residue No</th> <th>Atom Name</th> <th>Distance (in Å)</th> </tr> </thead> <tbody> <tr> <td>IMI</td> <td>N1</td> <td>SER</td> <td>70</td> <td>OG</td> <td>3.4</td> </tr> <tr> <td>IMI</td> <td>N1</td> <td>SER</td> <td>130</td> <td>OG</td> <td>3.5</td> </tr> <tr> <td>IMI</td> <td>N2</td> <td>THR</td> <td>237</td> <td>OG1</td> <td>3.7</td> </tr> <tr> <td>IMI</td> <td>N3</td> <td>THR</td> <td>216</td> <td>O</td> <td>3.05</td> </tr> <tr> <td>IMI</td> <td>N3</td> <td>GLU</td> <td>268</td> <td>OE2</td> <td>2.83</td> </tr> <tr> <td>IMI</td> <td>N3</td> <td>ARG</td> <td>220</td> <td>NE</td> <td>3.6</td> </tr> <tr> <td>IMI</td> <td>O16</td> <td>THR</td> <td>237</td> <td>N</td> <td>3.1</td> </tr> <tr> <td>IMI</td> <td>O19</td> <td>LYS</td> <td>73</td> <td>NZ</td> <td>2.9</td> </tr> <tr> <td>IMI</td> <td>O18</td> <td>LYS</td> <td>234</td> <td>NZ</td> <td>3.2</td> </tr> </tbody> </table>	Ligand	Atom Name	Residue Name	Residue No	Atom Name	Distance (in Å)	IMI	N1	SER	70	OG	3.4	IMI	N1	SER	130	OG	3.5	IMI	N2	THR	237	OG1	3.7	IMI	N3	THR	216	O	3.05	IMI	N3	GLU	268	OE2	2.83	IMI	N3	ARG	220	NE	3.6	IMI	O16	THR	237	N	3.1	IMI	O19	LYS	73	NZ	2.9	IMI	O18	LYS	234	NZ	3.2
Ligand	Atom Name	Residue Name	Residue No	Atom Name	Distance (in Å)																																																											
IMI	N1	SER	70	OG	3.4																																																											
IMI	N1	SER	130	OG	3.5																																																											
IMI	N2	THR	237	OG1	3.7																																																											
IMI	N3	THR	216	O	3.05																																																											
IMI	N3	GLU	268	OE2	2.83																																																											
IMI	N3	ARG	220	NE	3.6																																																											
IMI	O16	THR	237	N	3.1																																																											
IMI	O19	LYS	73	NZ	2.9																																																											
IMI	O18	LYS	234	NZ	3.2																																																											

^aThe K_i values were correlated with the molecular docking experiment. All interactions with their distances are tabulated in separate columns for each of the inhibitors.

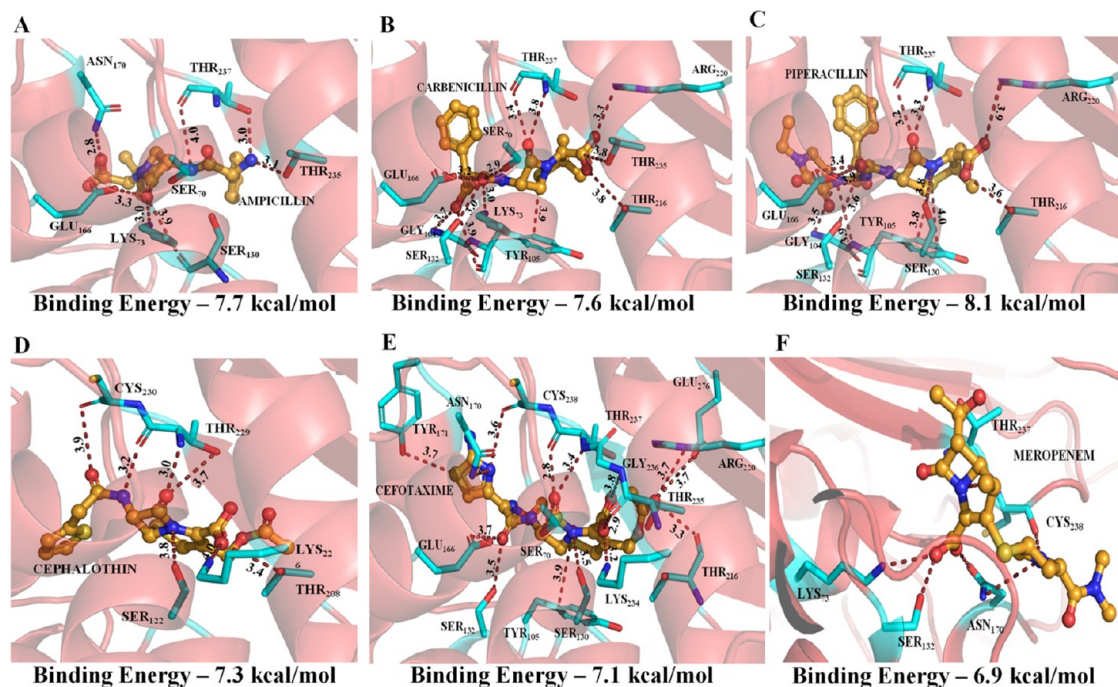


Figure 3. Molecular docking analysis of Ftu-1 with different substrates and inhibitors: All the hydrogen bonding interactions of the enzyme's amino acid residues and substrate atoms are highlighted with red dashes and their distances in the picture. (A) Ftu-1-Ampicillin complex, (B) Ftu-1-Carbenicillin complex, (C) Ftu-1-Piperacillin complex, (D) Ftu-1-Cephalothin complex, (E) Ftu-1-Cefotaxime complex, and (F) Ftu-1-Meropenem complex.

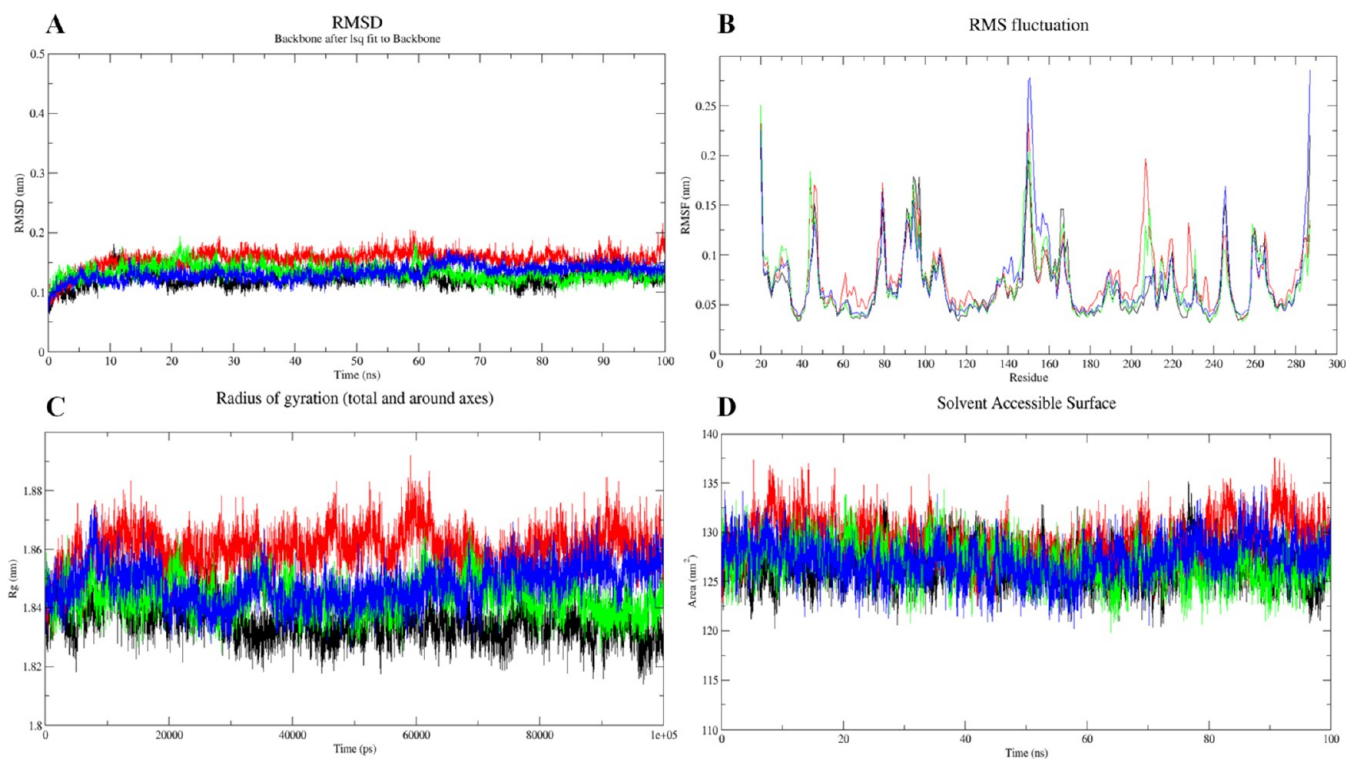


Figure 4. Molecular dynamics simulation analysis of Ftu-1-Apo and its complexes with ampicillin, cephalothin, and meropenem. (A) Time evolution backbone RMSD profiles of Ftu-1-Apo, Ftu-1-ampicillin, Ftu-1-cephalothin, and Ftu-1-meropenem complexes from the MD simulation trajectory. (B) RMSF profiles of Ftu-1-Apo, Ftu-1-ampicillin, Ftu-1-cephalothin, and Ftu-1-meropenem complexes as a function of residue number over the MD simulation trajectories. (C) Rg of $C\alpha$ atoms for Ftu-1-Apo, Ftu-1-ampicillin, Ftu-1-cephalothin, and Ftu-1-meropenem complexes during MD simulations as a function of time. (D) SASA analysis of Ftu-1-Apo, Ftu-1-ampicillin, Ftu-1-cephalothin, and Ftu-1-meropenem complexes during MD simulations as a function of time. Ftu-1-Apo is denoted in black, Ftu-1-ampicillin in red, Ftu-1-cephalothin in green, and Ftu-1-meropenem in blue.

Ftu-1. All of the MBIs clavulanic acid, sulbactam, and tazobactam show excellent inhibitory potentials of 30.68, 21.12, and 1.19 μM , respectively. Molecular docking against these MBIs with Ftu-1 shows us that two catalytic serine residues, ser70 and ser130, interact with these inhibitors, suggesting the unique behaviors of MBIs targeting the cross-linking of two serine residues and inactivating the enzyme. The inhibition kinetics result correlates with molecular docking studies and binding energy studies. Clavulanic acid shows a binding energy of -5.7 kcal/mol, a value lower than that of sulbactam (-6.4 kcal/mol) and tazobactam (-6.6 kcal/mol). The steady-state kinetic analysis shows us that carbapenems are not susceptible to Ftu-1 β -lactamase; this draws our attention to checking the inhibitory potential of carbapenems. Meropenem shows significant inhibitory potential with a k_i value of 1.53 μM compared to imipenem with a k_i value of 73.76 μM . Also, our molecular docking study found that imipenem has a lower binding energy (-6.4 kcal/mol) than meropenem (-6.9 kcal/mol) (Table 5).

Molecular Docking with Different β -Lactam Substrates. The selected penicillin group (ampicillin, carbenicillin, piperacillin), cephalosporin antibiotics (cephalothin, cefotaxime), and meropenem were tested, and we found that the binding energy of ampicillin is higher, which correlates with steady-state kinetics data. We found that the enzyme turnover number of piperacillin is higher in the steady-state kinetics experiment. The binding energy of piperacillin is -8.1 kcal/mol (highest among all of the tested antibiotics), suggesting significantly strong binding. The k_{cat}/K_m value of cephalothin is lower than penicillin; we also get a lower binding energy for cephalothin (-7.3 kcal/mol) compared to other penicillins, such as ampicillin and carbenicillin with -7.7 and -7.6 kcal/mol, respectively. Among carbapenems, imipenem and meropenem were tested against Ftu-1 β -lactamase; the binding energy of imipenem is lower (-6.4 kcal/mol) than that of meropenem (-6.9 kcal/mol), which also correlates with the inhibition kinetics value we obtained from inhibition kinetics data. The lower binding of imipenem may influence the k_i value of imipenem higher than the meropenem. All of the molecular dockings with represented figures are presented in Figure 3; all of the residues and atoms interacting with the ligand and their distances are tabulated in Tables S3–S8.

Overall Stability, Structural Flexibility, and Compactness of Ftu-1-Substrate Complexes. The Ftu-1-apo, Ftu-1-ampicillin, Ftu-1-cephalothin, and Ftu-1-meropenem complexes were analyzed for the structural and dynamic changes in respective MD simulation trajectories. The backbone RMSDs calculated for the 100 ns simulations displayed that all of the complexes converged well and did not deviate drastically from their starting structure during the simulations (Figure 4A). When inspected closely, it was found that Ftu-1-apo shows the lowest RMSD value of 0.123 nm. The binding of the substrate enhances the RMSD values. Among the three complexes tested, Ftu-1-ampicillin showed a higher RMSD value of 0.155 nm, and Ftu-1-cephalothin and Ftu-1-meropenem exhibited RMSDs of 0.133 and 0.132 nm, respectively, and this suggested that the Ftu-1-cephalothin and Ftu-1-meropenem complexes have undergone significant stable dynamics among all of the complexes. Next, the structural flexibilities of the Ftu-1 substrate complexes were examined using per-residue RMSF analysis (Figure 4B). It was found that all of the Ftu-1 substrate complexes exhibited a higher RMSF profile than Ftu-1-apo. The average RMSF value

of Ftu-1 apo is 0.068 nm, which is lower than the values of Ftu-1-ampicillin, Ftu-1-cephalothin, and Ftu-1-meropenem complexes with 0.077, 0.071, and 0.073 nm, respectively. The increase in fluctuation may be achieved due to the influence of ligand binding. It was also found that Ftu-1-ampicillin exhibited a spike in fluctuation at ser70, lys73, and ser130 residues (Ftu-1-apo RMSFs of 0.054, 0.036, and 0.05 nm, respectively, for ser70, lys73, and ser13, respectively, and RMSF values fluctuate to 0.082, 0.059, and 0.061 nm for the Ftu-1-ampicillin complex). The RMSF values of these catalytic residues do not fluctuate much for the other complexes. Another primary catalytic residue, glu166, fluctuates at 0.13 nm for the Ftu-1-meropenem complex compared to Ftu-1-apo of 0.101 nm. One of the observations that we also found is that the Ftu-1 complexes decrease the fluctuation around the omega loop, which suggests that the binding of the substrate stabilizes the omega loop (average RMSF value of the omega loop is 0.093 for Ftu-1-apo, 0.082 for Ftu-1-ampicillin, 0.090 for Ftu-1-cephalothin, and 0.091 for Ftu-1-meropenem). The Ftu-1 substrate complexes were then examined for compactness during MD simulations (Figure 4C). We found that Ftu-1-ampicillin exhibited a higher Rg of C α atoms (average of 1.860 nm) compared to Ftu-1-apo of 1.835 nm, Ftu-1-cephalothin of 1.843, and Ftu-1-meropenem of 1.847 nm. It indicates that Ftu-1-cephalothin and Ftu-1-meropenem have undergone less compact structural dynamics than the other complexes. This observation was coherent with the backbone RMSD measurements for Ftu-1-substrate complexes. The SASA analysis (Figure 4D) is also consistent with the RMSD data that Ftu-1-ampicillin shows a higher SASA of 129.17 nm² compared to the other complexes Ftu-1-cephalothin (126.8 nm²), Ftu-1-meropenem (127.2 nm²), and Ftu-1-apo (126.68 nm²).

Hydrogen Bonds Formed between Ftu-1 and Its Substrate Complexes and Interatomic Distance between Catalytic Residues and Substrates. The hydrogen bonds formed between the substrates and Ftu-1 and the intermolecular ones were computed during the 100 ns MD simulations. It was found that all three complexes share an almost similar number of hydrogen bonds throughout the simulation run. These results conclude the strong binding of substrates to Ftu-1 (Figure S4A–S4C). Additional information on the dynamics of the catalytic residues of Ftu-1 was obtained by computing the distance between the residues ser70, lys73, and glu166 with the substrates. First, the distance between the ser70-OG atom and the carbonyl carbon of each substrate revealed that the distances remained stable in all of the complexes. No significant fluctuation was observed (Figure S4D–S4F). Second, the distance between the lys73-NZ atom and the ser70-OG atom revealed that Ftu-1-meropenem exhibited the lowest average distance. We see significant fluctuation in the average distance in the cases of Ftu-1-ampicillin and Ftu-1-cephalothin complexes (Figure S4G–S4I). Third, the distance during MD simulations between glu166-OE2 and the carbonyl carbon of each substrate revealed that Ftu-1-ampicillin and Ftu-1-meropenem were the two that exhibited stable average distances. At the same time, Ftu-1-cephalothin experienced significant fluctuation after a 60 ns simulation run (Figure S4J–S4L). Generally, it was tracked that each of the substrates ampicillin, cephalothin, and meropenem maintained stable associations with the active site of Ftu-1, laying out the significance of these key interactions.

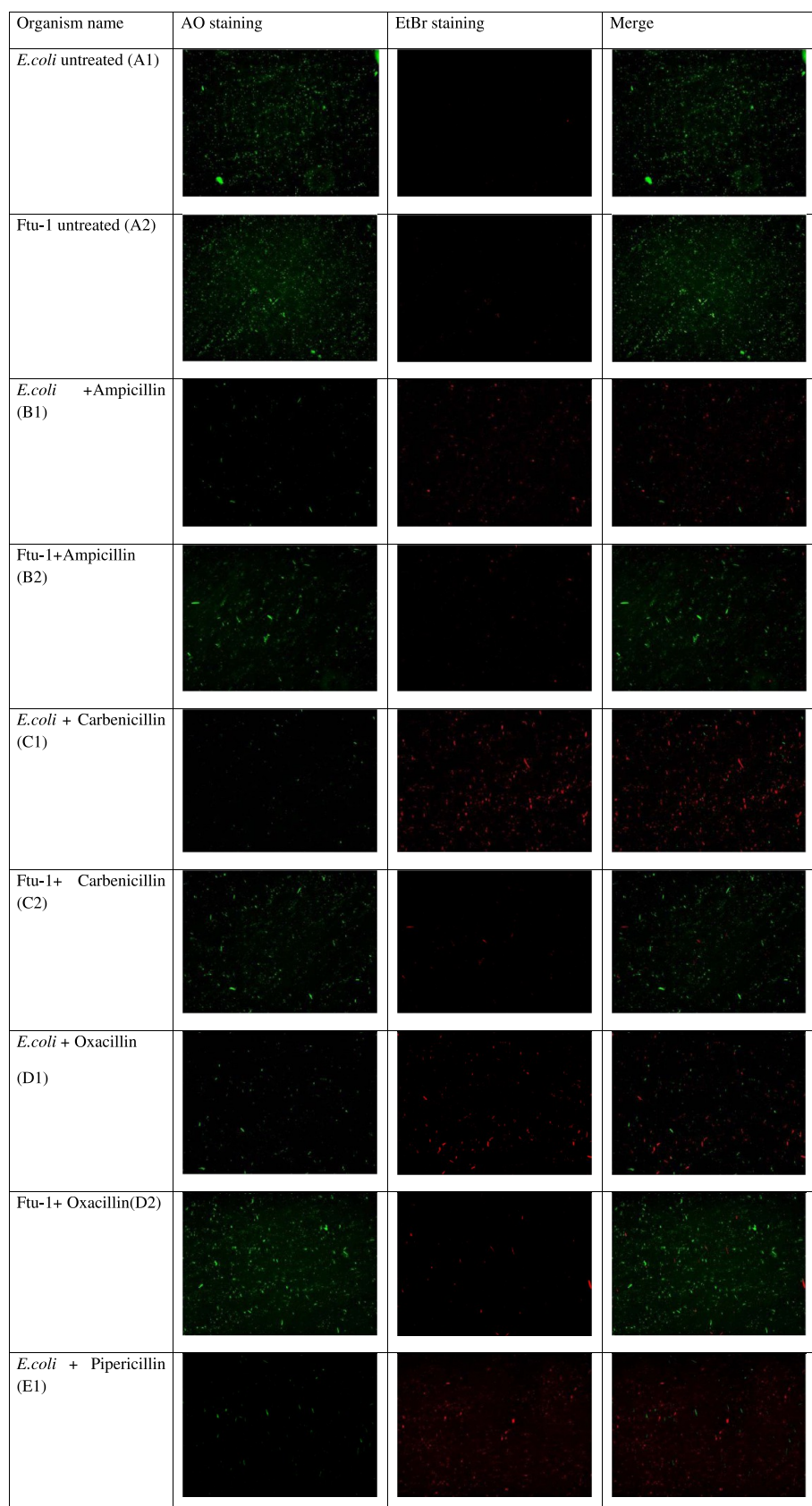


Figure 5. continued

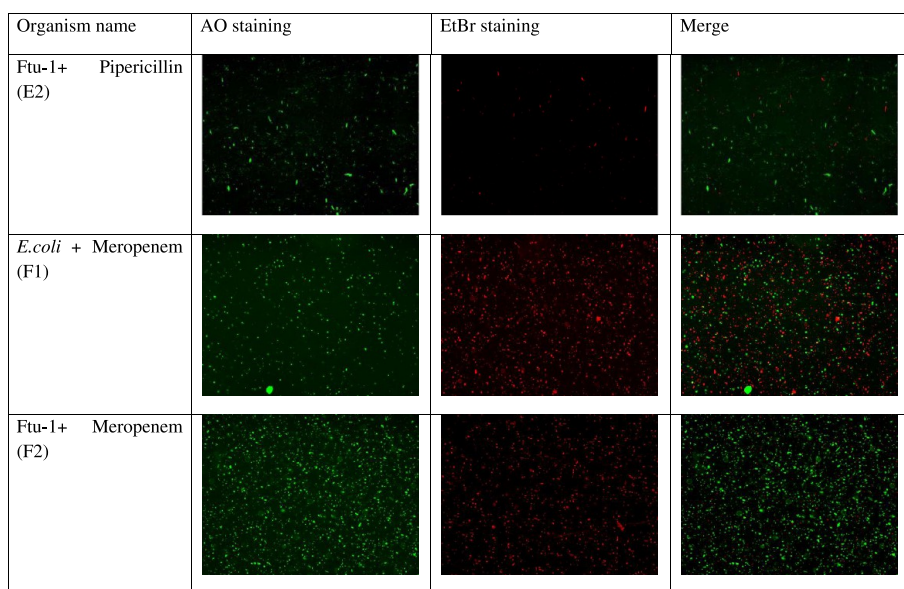


Figure 5. Live/dead cell visualization using fluorescence microscopy: Representative fluorescence microscopy images of AO/EB-based dual staining of *E. coli* (control) and Ftut-1 expressing bacterial cell (A1–A2) after incubation with ampicillin (B1–B2), carbenicillin (C1–C2), oxacillin (D1–D2), piperacillin (E1–E2), and meropenem (F1–F20 to determine the proportion of live and dead cells and to correlate the resistance profile shown by the bacteria).

Antimicrobial Susceptibility Test. Clones expressing the Ftut-1 gene show significant resistance to penicillin and narrow-generation cephalosporin drugs as measured by disk diffusion and MIC of various antibiotics. The Ftut-1 clone does not elevate the MIC for carbapenems tested; the respective zone diameter of the carbapenem-treated clone also suggests that the Ftut-1-expressing clone remains susceptible to carbapenems. Fluorescence spectroscopy also showed that the Ftut-1 clone seems to be living in AO/EB staining and is visualized as green. Carbapenem-treated Ftut-1 clones stain red and remain dead when imaged in fluorescence microscopy, which also suggests susceptibility toward carbapenems. All of the values corresponding to the zone of inhibition with the MIC value are tabulated in Table S9, and the fluorescence microscopy-based image is shown in Figure 5. We have quantitated all of the images coming from fluorescence microscopy imaging and obtained the live/dead ratio (Figure S5) against wild-type *E. coli* and Ftut-1 expressing bacteria when treated with different antibiotics. Both of the cells, when left untreated, showed similar live/dead ratios and are referred to as ns (non-significant). We also obtained very low live/dead ratios when wild-type *E. coli* were treated with different antibiotics, which suggests that *E. coli* was susceptible to different antibiotics, whereas we observed a higher live/dead ratio against Ftut-1, suggesting resistance against the tested antibiotics.

CONCLUSIONS

Structurally, all of the carbapenemases have two conserved cysteine residues at position 69 and position 238. Ftut-1 β -lactamase from *Francisella tularensis* contains all of the structural features of a class A carbapenemase, including the conserved disulfide bond. Ftut-1 belongs to class A β -lactamase with a very distinct class, mainly related to FPH-1, a class A carbapenemase from another *Francisella* organism. Ftut-1 β -lactamase was cloned, purified, and biophysically characterized. The melting temperature of Ftut-1 was around 63 °C, which is significantly higher than other class A β -lactamases like TEM,

SHV, Bla1, BlaC, KPC, and CTX-M-14. The T_m of these enzymes typically ranges from 50 to 55 °C (Table 6).

Table 6. Comparative T_m of Different Class A β -Lactamases

name of the enzyme	organism name	T_m of the enzyme (°C)	technique used	reference
Ftut-1	<i>Francisella tularensis</i>	63.0	CD and DSC	this study
TEM	<i>Escherichia coli</i>	51.6	DSC	58
SHV-1	<i>Klebsiella pneumoniae</i>	54.2	CD	59
KPC 2	<i>Klebsiella pneumoniae</i>	54.7	DSF	60
KPC 3	<i>Klebsiella pneumoniae</i>	55.1	DSF	60
PenP	<i>Burkholderia cepacia</i>	56.0	CD	61
BlaC	<i>Mycobacterium tuberculosis</i>	60.0	CD	37
Bla1	<i>Bacillus anthracis</i>	56.02	CD	62
CTX-M-9	<i>Escherichia coli</i>	48.9	CD	63
CTX-M-14	<i>Escherichia coli</i>	50.9	CD	63
CTX-M-16	<i>Escherichia coli</i>	47.6	CD	63
CTX-M-27	<i>Escherichia coli</i>	49.9	CD	63
AmpC	<i>Escherichia coli</i>	54.6	CD	64

We assume to reduce the disulfide bond by incubating the enzyme with 1 mM DTT; the melting temperature is around 61 °C. The 2 °C decreases in the melting point may result in reduced structural stability associated with the disulfide bond (Figure 6). We have measured the hydrolysis parameters of Ftut-1. Ftut-1 efficiently cleaves narrow-generation cephalosporins and penicillin. Molecular docking analyses also correlate with the enzyme parameter data. Penicillin shows a significantly higher binding potential than cephalosporins. Having all of the characteristics of class A carbapenemases, Ftut-1 does not show any resistance toward carbapenems. MBIs show significant inhibition toward Ftut-1, and a molecular

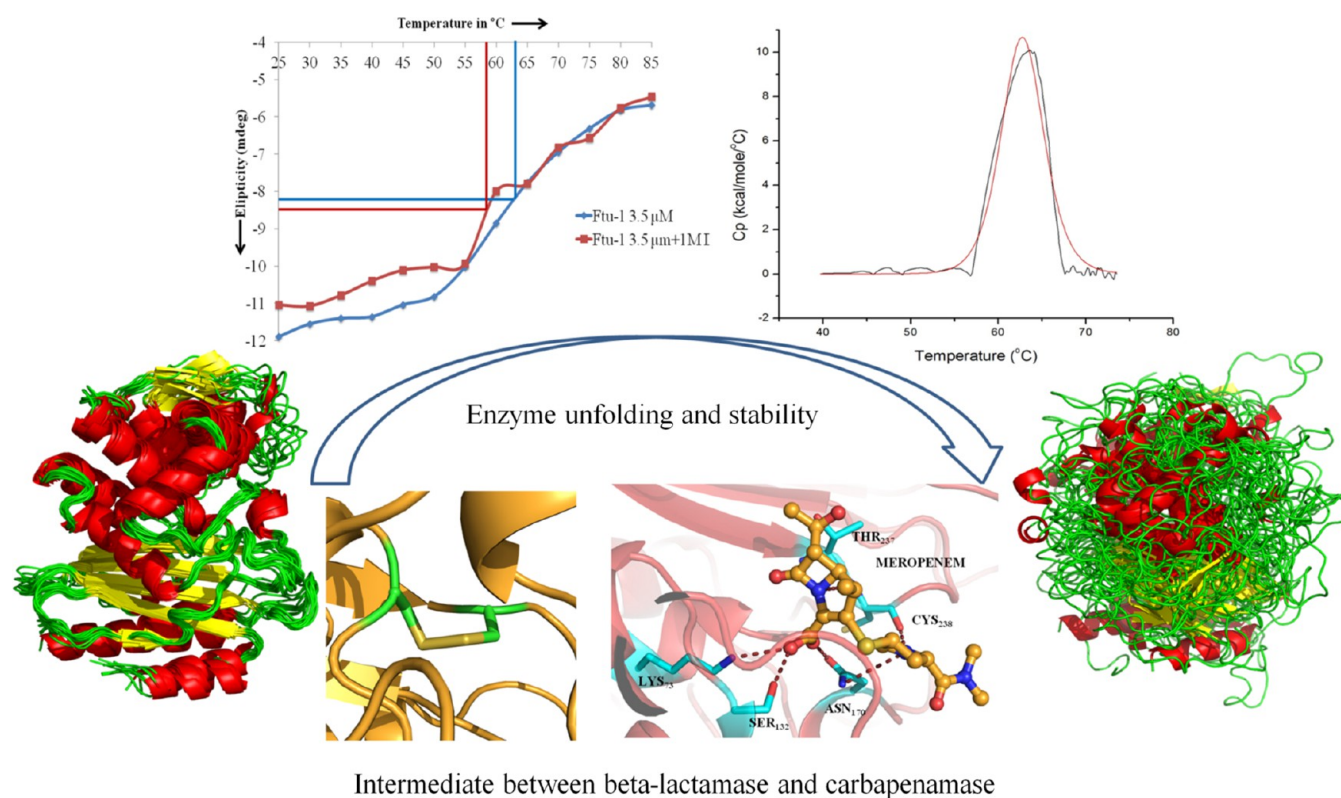


Figure 6. Proposed model to describe the unique, distinctive class of FtU-1 β -lactamase; the particular enzyme also elevated the melting temperature compared to other members of this class.

docking study suggests a typical mechanism of inhibition by cross-linking two active site serine residues. Carbapenems like meropenem and imipenem also show inhibition with significant k_i values. Our MIC and live bacterial killing imaging study also demonstrate that carbapenems are not susceptible to clones expressing FtU-1 β -lactamase.

■ ASSOCIATED CONTENT

SI Supporting Information

The Supporting Information is available free of charge at <https://pubs.acs.org/doi/10.1021/acsbiochemau.2c00044>.

ftu1_300_1 (AVI)

FTU1_500_1 (AVI)

Three-dimensional representation of FtU-1 β -lactamase; MD simulation analysis of FtU-1 apo at different temperatures; biophysical and biochemical bases of stability and functionality of FtU-1 β -lactamase; hydrogen bonds and interatomic distance between catalytic FtU-1 residues and substrates; unfolding pathway of FtU-1 β -lactamase; kinetic rate profiling with the influence of salt concentration; molecular docking analysis of FtU-1 with ampicillin; and antimicrobial susceptibility of the β -lactam antibiotic against FtU-1 containing BL21 (DE3) and BL21 (DE3) as controls (PDF)

■ AUTHOR INFORMATION

Corresponding Author

Saugata Hazra – Department of Bioscience and Bioengineering, Indian Institute of Technology Roorkee, Roorkee 247667, India; Centre of Nanotechnology, Indian Institute of

Technology Roorkee, Roorkee 247667, India; orcid.org/0000-0002-3074-1534; Email: saugata.iitk@gmail.com, saugata.hazra@bt.iitr.ac.in

Authors

Sourya Bhattacharya – Department of Bioscience and Bioengineering, Indian Institute of Technology Roorkee, Roorkee 247667, India

Vivek Junghare – Department of Bioscience and Bioengineering, Indian Institute of Technology Roorkee, Roorkee 247667, India; orcid.org/0000-0002-7952-2092

Mousumi Hazra – Department of Botany and Microbiology, Gurukula Kangri (Deemed to be University), Haridwar 249404 Uttarakhand, India; orcid.org/0000-0001-5791-7993

Niteesh Kumar Pandey – Department of Bioscience and Bioengineering, Indian Institute of Technology Roorkee, Roorkee 247667, India

Abirral Mukherjee – Department of Bioscience and Bioengineering, Indian Institute of Technology Roorkee, Roorkee 247667, India

Kunal Dhankhar – Department of Bioscience and Bioengineering, Indian Institute of Technology Roorkee, Roorkee 247667, India

Neeladrisingha Das – Department of Bioscience and Bioengineering, Indian Institute of Technology Roorkee, Roorkee 247667, India

Partha Roy – Department of Bioscience and Bioengineering, Indian Institute of Technology Roorkee, Roorkee 247667, India

Ramesh Chandra Dubey – Department of Botany and Microbiology, Gurukula Kangri (Deemed to be University), Haridwar 249404 Uttarakhand, India

Complete contact information is available at:

<https://pubs.acs.org/10.1021/acsbiomedchemau.2c00044>

Author Contributions

S.B.: Investigation, writing—original draft. V.J.: Formal analysis, in silico study. M.H.: Protein dynamics, analysis of protein dynamics. N.K.P.: Formal analysis, methodologies. A.M.: Enzyme kinetics study. K.D.: Biochemical investigation and analysis. N.D.: Fluorescent microscopy, P.R.: Analysis of fluorescent microscopy. R.C.D.: Review and editing. S.H.: Supervision, fund acquisition, conceptualization, methodology, software, review and editing. CRediT: **Sourya Bhattacharya** investigation (equal), writing-original draft (equal); **Vivek Junghare** formal analysis (equal), methodology (equal); **Mousumi Hazra** formal analysis (equal); **Niteesh Kumar Pandey** formal analysis (equal), methodology (equal); **Abirlal Mukherjee** formal analysis (equal); **Kunal Dhankhar** formal analysis (equal); **Neeladrisingha Das** formal analysis (equal); **Partha Roy** formal analysis (equal); **Ramesh Chandra Dubey** writing-review & editing (equal); **Saugata Hazra** conceptualization (equal), funding acquisition (equal), methodology (equal), project administration (equal), software (equal), supervision (equal), validation (equal), writing-review & editing (equal).

Notes

The authors declare no competing financial interest.

The separate supporting information contains different biophysical, biochemical, and dynamic characterization data of Ftu-1 β -lactamase, mainly focusing on the effect of stability toward different physicochemical parameters. It also contains a quantitative analysis of the bacterial resistance pattern as well as different interaction parameters against different substrates and inhibitors using molecular docking.

ACKNOWLEDGMENTS

A part of the work was conducted in the Department of Biotechnology central facility and Bioinformatics Center, Department of Biotechnology, IIT Roorkee. Financial support through ICMR (Indian Council of Medical Research) sanction number BIC/12(15)/2014, FIG (IITR) sanction number FIG 100671/14, SERB (Science and Engineering Research Board, India) sanction number YSS/2014/000492, SPARC (Scheme for Promotion of Academic and Research Collaboration, Minister of Human Resource development, India) sanction number SPARC/2018-2019/8/SL(IN), and TIH IITR (technology innovation hub (iHUB)) sanction number TIH/CS/04 to SH are gratefully acknowledged.

REFERENCES

- Pandey, N.; Cascella, M. Beta Lactam Antibiotics. In *Antibiotic Discovery and Development*; StatPearls Publishing, 2022; pp 79–117.
- Bush, K.; Bradford, P. A. β -Lactams and β -Lactamase Inhibitors: An Overview. *Cold Spring Harbor Perspect. Med.* **2016**, *6*, No. a025247.
- Tooke, C. L.; Hinchliffe, P.; Bragginton, E. C.; Colenso, C. K.; Hirvonen, V. H. A.; Takebayashi, Y.; Spencer, J. β -Lactamases and β -Lactamase Inhibitors in the 21st Century. *J. Mol. Biol.* **2019**, *431*, 3472–3500.
- Rawat, D.; Nair, D. Extended-spectrum β -lactamases in Gram Negative Bacteria. *J. Global Infect. Dis.* **2010**, *2*, No. 263.
- Paterson, D. L.; Bonomo, R. A. Extended-Spectrum β -Lactamases: a Clinical Update. *Clin. Microbiol. Rev.* **2005**, *18*, 657–686.
- Hawkey, P. M.; Livermore, D. M. Carbapenem antibiotics for serious infections. *BMJ.* **2012**, *344*, No. e3236.
- Papp-Wallace, K. M.; Endimiani, A.; Taracila, M. A.; Bonomo, R. A. Carbapenems: Past, Present, and Future. *Antimicrob. Agents Chemother.* **2011**, *55*, 4943–4960.
- Codjoe, F. S.; Donkor, E. S. Carbapenem Resistance: A Review. *Med. Sci.* **2018**, *6*, No. 1.
- Meletis, G. Carbapenem resistance: overview of the problem and future perspectives. *Ther. Adv. Infect. Dis.* **2016**, *3*, 15–21.
- Queenan, A. M.; Bush, K. Carbapenemases: the Versatile β -Lactamases. *Clin. Microbiol. Rev.* **2007**, *20*, 440–458.
- Antunes, N. T.; Lamoureux, T. L.; Toth, M.; Stewart, N. K.; Frase, H.; Vakulenko, S. B. Class D β -lactamases: Are they all carbapenemases? *Antimicrob. Agents Chemother.* **2014**, *58*, 2119–2125.
- Palzkill, T. Metallo- β -lactamase structure and function. *Ann. N. Y. Acad. Sci.* **2013**, *1277*, 91–104.
- Walther-Rasmussen, J.; Høiby, N. Class A carbapenemases. *J. Antimicrob. Chemother.* **2007**, *60*, 470–482.
- Naas, T.; Dortet, L.; Iorga, B. I. Structural and Functional Aspects of Class A Carbapenemases. *Curr. Drug Targets.* **2016**, *17*, 1006–1028.
- Queenan, A. M.; Bush, K. Carbapenemases: the versatile beta-lactamases. *Clin. Microbiol. Rev.* **2007**, *20*, 440–458.
- Nordmann, P.; Naas, T.; Poirel, L. Global spread of Carbapenemase-producing Enterobacteriaceae. *Emerging Infect. Dis.* **2011**, *17*, 1791–1798.
- Naas, T.; Oueslati, S.; Bonnin, R. A.; Dabos, M. L.; Zavala, A.; Dortet, L.; Retailleau, P.; Iorga, B. I. Beta-lactamase database (BLDB)—structure and function. *J. Enzyme Inhib. Med. Chem.* **2017**, *32*, 917–919.
- Sievers, F.; Wilm, A.; Dineen, D.; Gibson, T. J.; Karplus, K.; Li, W.; Lopez, R.; McWilliam, H.; Remmert, M.; Söding, J.; Thompson, J. D.; Higgins, D. G. Fast, scalable generation of high-quality protein multiple sequence alignments using Clustal Omega. *Mol. Syst. Biol.* **2011**, *7*, No. 539.
- Jones, D. T.; Taylor, W. R.; Thornton, J. M. The rapid generation of mutation data matrices from protein sequences. *Bioinformatics* **1992**, *8*, 275–282.
- Kumar, S.; Stecher, G.; Li, M.; Nknyaz, C.; Tamura, K. MEGA X: Molecular Evolutionary Genetics Analysis across Computing Platforms. *Mol. Biol. Evol.* **2018**, *35*, 1547–1549.
- Hess, B.; Kutzner, C.; van der Spoel, D.; Lindahl, E. GROMACS 4: Algorithms for highly efficient, load-balanced, and scalable molecular simulation. *J. Chem. Theory Comput.* **2008**, *4*, 435–447.
- Huang, J.; Sun, C.; Mitchell, O.; Ng, N.; Wang, Z. N.; Boutis, G. S. On the inverse temperature transition and development of an entropic elastomeric force of the elastin mimetic peptide [LGGVG]₃. *J. Chem. Phys.* **2012**, *136*, No. 085101.
- Pronk, S.; Páll, S.; Schulz, R.; Larsson, P.; Bjelkmar, P.; Apostolov, R.; Shirts, M. R.; Smith, J. C.; Kasson, P. M.; van der Spoel, D.; Hess, B.; Lindahl, E. GROMACS 4.5: a high-throughput and highly parallel open source molecular simulation toolkit. *Bioinformatics* **2013**, *29*, 845–854.
- Kundu, S.; Roy, D. Comparative structural studies of psychrophilic and mesophilic protein homologues by molecular dynamics simulation. *J. Mol. Graphics Modell.* **2009**, *27*, 871–880.
- Weber, W.; Hünenberger, P. H.; Andrew McCammon, J. Molecular dynamics simulations of a polyalanine octapeptide under ewald boundary conditions: influence of artificial periodicity on peptide conformation. *J. Phys. Chem. B* **2000**, *104*, 3668–3675.

- (26) Hess, B.; Bekker, H.; Berendsen, H. J. C.; Fraaije, J. G. E. M. LINCS: A Linear Constraint Solver for Molecular Simulations. *J. Comput. Chem.* **1997**, *18*, 1463–1472.
- (27) Darden, T.; Perera, L.; Li, L.; Lee, P. New tricks for modelers from the crystallography toolkit: the particle mesh Ewald algorithm and its use in nucleic acid simulations. *Structure* **1999**, *7*, R55–R60.
- (28) DeLano, W. L. *The PyMOL Molecular Graphics System*; Delano Scientific: San Carlos, 2002.
- (29) Graphing with Gnuplot and Xmgr | Linux Journal. [cited 2022 Jun 28]. Available from: <https://www.linuxjournal.com/article/1218>.
- (30) MathWorks Introduces Major New Release of MATLAB - MATLAB & Simulink [Internet]. Available from: <https://www.mathworks.com/company/newsroom/mathworks-introduces-major-new-release-of-matlab.html>. 2014, Oct 8.
- (31) Humphrey, W.; Dalke, A.; Schulten, K. VMD: visual molecular dynamics. *J. Mol. Graphics* **1996**, *14*, 33–38.
- (32) Christov, C.; Gabriel, S.; Atanasov, B.; Fleischhauer, J. Calculation of the CD spectrum of class A β -lactamase from *Escherichia coli* (TEM-1). *Z. Naturforsch., A* **2001**, *56*, 757–760.
- (33) Bhattacharya, S.; Junghare, V.; Pandey, N. K.; Ghosh, D.; Patra, H.; Hazra, S. An insight into the complete biophysical and biochemical characterization of novel class A beta-lactamase (Bla1) from *Bacillus anthracis*. *Int. J. Biol. Macromol.* **2020**, *145*, 510–526.
- (34) Hart, K. M.; Ho, C. M. W.; Dutta, S.; Gross, M. L.; Bowman, G. R. Modelling proteins' hidden conformations to predict antibiotic resistance. *Nat. Commun.* **2016**, *7*, No. 12965.
- (35) Kuwajima, K.; Nitta, K.; Yoneyama, M.; Sugai, S. Three-state denaturation of alpha-lactalbumin by guanidine hydrochloride. *J. Mol. Biol.* **1976**, *106*, 359–373.
- (36) Durowoju, I. B.; Bhandal, K. S.; Hu, J.; Carpick, B.; Kirkitadze, M. Differential Scanning Calorimetry - A Method for Assessing the Thermal Stability and Conformation of Protein Antigen. *J. Visualized Exp.* **2017**, *2017*, No. e55262.
- (37) Bhattacharya, S.; Junghare, V.; Pandey, N. K.; Baidya, S.; Agarwal, H.; Das, N.; et al. Variations in the SDN Loop of Class A Beta-Lactamases: A Study of the Molecular Mechanism of BlaC (*Mycobacterium tuberculosis*) to Alter the Stability and Catalytic Activity Towards Antibiotic Resistance of MBIs. *Front. Microbiol.* **2021**, *12*, No. 2685.
- (38) Quartararo, C. E.; Hazra, S.; Hadi, T.; Blanchard, J. S. Structural, kinetic and chemical mechanism of isocitrate dehydrogenase-1 from *Mycobacterium tuberculosis*. *Biochemistry* **2013**, *52*, 1765–1775.
- (39) Hazra, S.; Kurz, S. G.; Wolff, K.; Nguyen, L.; Bonomo, R. A.; Blanchard, J. S. Kinetic and Structural Characterization of the Interaction of 6-Methylidene Penem 2 with the β -Lactamase from *Mycobacterium tuberculosis*. *Biochemistry* **2015**, *54*, 5657–5664.
- (40) Hazra, S.; Xu, H.; Blanchard, J. S. Tebipenem, a New Carbapenem Antibiotic, Is a Slow Substrate That Inhibits the β -Lactamase from *Mycobacterium tuberculosis*. *Biochemistry* **2014**, *53*, 3671–3678.
- (41) Faheem, M.; Rehman, M. T.; Danishuddin, M.; Khan, A. U. Biochemical characterization of CTX-M-15 from Enterobacter cloacae and designing a novel non- β -lactam- β -lactamase inhibitor. *PLoS One* **2013**, *8*, No. e56926.
- (42) Bhattacharya, S.; Padhi, A. K.; Junghare, V.; Das, N.; Ghosh, D.; Roy, P.; et al. Understanding the molecular interactions of inhibitors against Bla1 beta-lactamase towards unraveling the mechanism of antimicrobial resistance. *Int. J. Biol. Macromol.* **2021**, *177*, 337–350.
- (43) Kurz, S. G.; Hazra, S.; Bethel, C. R.; Romagnoli, C.; Caselli, E.; Prati, F.; et al. Inhibiting the β -Lactamase of *Mycobacterium tuberculosis* (Mtb) with Novel Boronic Acid Transition-State Inhibitors (BATsIs). *ACS Infect. Dis.* **2016**, *1*, 234–242.
- (44) Kurz, S. G.; Wolff, K. A.; Hazra, S.; Bethel, C. R.; Hujer, A. M.; Smith, K. M.; et al. Can Inhibitor-Resistant Substitutions in the *Mycobacterium tuberculosis* β -Lactamase BlaC Lead to Clavulanate Resistance?: a Biochemical Rationale for the Use of β -Lactam- β -Lactamase Inhibitor Combinations. *Antimicrob. Agents Chemother.* **2013**, *57*, 6085–6096.
- (45) Xu, H.; Hazra, S.; Blanchard, J. S. NXL104 irreversibly inhibits the β -lactamase from *Mycobacterium tuberculosis*. *Biochemistry* **2012**, *51*, 4551–4557.
- (46) Mendelsohn, L. D. ChemDraw 8 ultra, windows and macintosh versions. *J. Chem. Inf. Comput. Sci.* **2004**, *44*, 2225–2226.
- (47) Schwede, T.; Kopp, J.; Guex, N.; Peitsch, M. C. SWISS-MODEL: An automated protein homology-modeling server. *Nucleic Acids Res.* **2003**, *31*, 3381–3385.
- (48) Trott, O.; Olson, A. J. AutoDock Vina: improving the speed and accuracy of docking with a new scoring function, efficient optimization and multithreading. *J. Comput. Chem.* **2010**, *31*, 455–461.
- (49) Huey, R.; Morris, G. M. *Using AutoDock 4 with AutoDocktools: a Tutorial*; The Scripps Research Institute, Molecular Graphics Laboratory: La Jolla, CA, USA, 2008; pp 54–56.
- (50) Emsley, P.; Cowtan, K. Coot: model-building tools for molecular graphics. *Acta Crystallogr., Sect. D: Biol. Crystallogr.* **2004**, *60*, 2126–2132.
- (51) Leber, Amy L. *Clinical Microbiology Procedures Handbook*; American Society for Microbiology, 2010.
- (52) M07: Dilution AST for Aerobically Grown Bacteria - CLSI. [cited 2022 Jun 28]. Available from: <https://clsi.org/standards/products/microbiology/documents/m07/>.
- (53) Bauer, A. W.; Kirby, W. M.; Sherris, J. C.; Turck, M. Antibiotic susceptibility testing by a standardized single disk method. *Am. J. Clin. Pathol.* **1966**, *45*, 493–496.
- (54) Radetsky, M.; Wheeler, R. C.; Roe, M. H.; Todd, J. K. Microtiter broth dilution method for yeast susceptibility testing with validation by clinical outcome. *J. Clin. Microbiol.* **1986**, *24*, 600–606.
- (55) Toth, M.; Vakulenko, V.; Antunes, N. T.; Frase, H.; Vakulenko, S. B. Class A Carbapenemase FPH-1 from *Francisella philomiragia*. *Antimicrob. Agents Chemother.* **2012**, *56*, 2852–2857.
- (56) Majiduddin, F. K.; Palzkill, T. Amino acid sequence requirements at residues 69 and 238 for the SME-1 beta-lactamase to confer resistance to beta-lactam antibiotics. *Antimicrob. Agents Chemother.* **2003**, *47*, 1062–1067.
- (57) Lamoureaux, T. L.; Vakulenko, V.; Toth, M.; Frase, H.; Vakulenko, S. B. A novel extended-spectrum β -lactamase, SGM-1, from an environmental isolate of *Sphingobium* sp. *Antimicrob. Agents Chemother.* **2013**, *57*, 3783–3788.
- (58) Wang, X.; Minasov, G.; Shoichet, B. K. Noncovalent interaction energies in covalent complexes: TEM-1 β -lactamase and β -lactams. *Proteins: Struct., Funct., Genet.* **2002**, *47*, 86–96.
- (59) Whitman, I. R.; Patel, V. V.; Soliman, E. Z.; Bluemke, D. A.; Praestgaard, A.; Jain, A.; Herrington, D.; Lima, J. A. C.; Kawut, S. M. Validity of the surface electrocardiogram criteria for right ventricular hypertrophy: the MESA-RV Study (Multi-Ethnic Study of Atherosclerosis-Right Ventricle). *J. Am. Coll. Cardiol.* **2014**, *63*, 672–681. Feb 25
- (60) Taracila, M. A.; Bethel, C. R.; Hujer, A. M.; Papp-wallace, K. M.; Barnes, M. D.; et al. Different Conformations Revealed by NMR Underlie Resistance to Ceftazidime / Avibactam and Susceptibility to Meropenem and Imipenem among D179Y Variants of KPC β -Lactamase. *Antimicrob. Agents Chemother.* **2022**, *66*, No. e02124-21.
- (61) Au, H. W.; Tsang, M. W.; So, P. K.; Wong, K. Y.; Leung, Y. C. Thermostable β -Lactamase Mutant with Its Active Site Conjugated with Fluorescein for Efficient β -Lactam Antibiotic Detection. *ACS Omega* **2019**, *4*, 20493–20502.
- (62) Bhattacharya, S.; Junghare, V.; Pandey, N. K.; Ghosh, D.; Patra, H.; Hazra, S. An insight into the complete biophysical and biochemical characterization of novel class A beta-lactamase (Bla1) from *Bacillus anthracis*. *Int. J. Biol. Macromol.* **2020**, *145*, 510–526.
- (63) Chen, Y.; Delmas, J.; Siro, J.; Shoichet, B.; Bonnet, R. Atomic Resolution Structures of CTX-M β -Lactamases: Extended Spectrum Activities from Increased Mobility and Decreased Stability. *J. Mol. Biol.* **2005**, *348*, 349–362.
- (64) Beadle, B. M.; McGovern, S. L.; Patera, A.; Shoichet, B. K. Functional analyses of AmpC β -lactamase through differential stability. *Protein Sci.* **1999**, *8*, 1816–1824.